Forum of Mathematics, Sigma (2017), Vol. 5, e18, 48 pages
doi:10.1017/fms.2017.10

MINIMALITY AND MUTATION-EQUIVALENCE OF POLYGONS

ALEXANDER KASPRZYK[1], BENJAMIN NILL[2] and THOMAS PRINCE[3]

[1] School of Mathematical Sciences, University of Nottingham, University Park, Nottingham NG7 2RD, UK;
email: a.m.kasprzyk@nottingham.ac.uk

[2] Fakultät für Mathematik, Otto-von-Guericke-Universität Magdeburg, Postschließfach 4120, 39016 Magdeburg, Germany;
email: benjamin.nill@ovgu.de

[3] Department of Mathematics, Imperial College London, 180 Queen's Gate, London SW7 2AZ, UK;
email: t.prince12@imperial.ac.uk

Received 1 April 2015; accepted 3 March 2017

Abstract

We introduce a concept of minimality for Fano polygons. We show that, up to mutation, there are only finitely many Fano polygons with given singularity content, and give an algorithm to determine representatives for all mutation-equivalence classes of such polygons. This is a key step in a program to classify orbifold del Pezzo surfaces using mirror symmetry. As an application, we classify all Fano polygons such that the corresponding toric surface is qG-deformation-equivalent to either (i) a smooth surface; or (ii) a surface with only singularities of type $1/3(1, 1)$.

1. Introduction

1.1. An introduction from the viewpoint of algebraic geometry and mirror symmetry. A *Fano polygon* P is a convex polytope in $N_{\mathbb{Q}} := N \otimes_{\mathbb{Z}} \mathbb{Q}$, where N is a rank-two lattice, with primitive vertices $\mathcal{V}(P)$ in N such that the origin is contained in its strict interior, $\mathbf{0} \in P^{\circ}$. A Fano polygon defines a toric surface X_P given by the *spanning fan* (also commonly referred to as the *face fan* or *central fan*) of P; that is, X_P is defined by the fan whose cones are spanned by the faces of P. The toric surface X_P has cyclic quotient singularities (corresponding to the

© The Author(s) 2017. This is an Open Access article, distributed under the terms of the Creative Commons Attribution licence (http://creativecommons.org/licenses/by/4.0/), which permits unrestricted re-use, distribution, and reproduction in any medium, provided the original work is properly cited.

Downloaded from https://www.cambridge.org/core. IP address: 185.31.154.38, on 21 Aug 2017 at 16:48:03, subject to the Cambridge Core terms of use, available at https://www.cambridge.org/core/terms. https://doi.org/10.1017/fms.2017.10

cones over the edges of P) and the anti-canonical divisor $-K_{X_P}$ is $\mathbb{Q}$-Cartier and ample. Hence X_P is a toric *del Pezzo surface*.

The simplest example of a toric del Pezzo surface is $\mathbb{P}^2$, corresponding, up to $\mathrm{GL}_2(\mathbb{Z})$-equivalence, to the triangle $P = \mathrm{conv}\{(1,0),(0,1),(-1,-1)\}$. It is well known that there are exactly five smooth toric del Pezzo surfaces, and that these are a subset of the sixteen toric Gorenstein del Pezzo surfaces (in bijective correspondence with the famous sixteen reflexive polygons described by Batyrev and Rabinowitz [7, 37]). More generally, if one bounds the *Gorenstein index* r (the smallest positive integer such that $-rK_{X_P}$ is Cartier) the number of possibilities is finite. Dais classified those toric del Pezzo surfaces with Picard rank one and $r \leqslant 3$ [15]. A general classification algorithm was presented in [28].

A new viewpoint on del Pezzo classification is suggested by mirror symmetry. We shall sketch this briefly; for details see [11]. An n-dimensional Fano variety X is expected to correspond, under mirror symmetry, to a Laurent polynomial $f \in \mathbb{C}[x_1^{\pm 1}, \ldots, x_n^{\pm 1}]$ [5, 8, 11, 12]. Under this correspondence, the regularized quantum period $\widehat{G}_X$ of X – a generating function for Gromov–Witten invariants – coincides with the classical period π_f of f – a solution of the associated Picard–Fuchs differential equation – given by

$$\pi_f(t) = \left(\frac{1}{2\pi i}\right)^n \int_{|x_1|=\cdots=|x_n|=1} \frac{1}{1-tf} \frac{dx_1}{x_1} \cdots \frac{dx_n}{x_n} = \sum_{k \geqslant 0} \mathrm{coeff}_1(f^k) t^k.$$

If a Fano variety X is mirror to a Laurent polynomial f then it is expected that X admits a degeneration to the singular toric variety X_P associated to the Newton polytope P of f.

In general there will be many (often infinitely many) different Laurent polynomials mirror dual to X, and hence many toric degenerations X_P. It is conjectured that these Laurent polynomials are related via birational transformations analogous to cluster transformations, which are called *mutations* [2, 17, 19, 20]. A mutation acts on the Newton polytope $P := \mathrm{Newt}(f) \subset N_{\mathbb{Q}}$ of a Laurent polynomial via 'rearrangement of Minkowski slices' (see Section 2.1), and on the dual polytope $P^* \subset M_{\mathbb{Q}}$, $M := \mathrm{Hom}(N, \mathbb{Z})$, via a piecewise-$\mathrm{GL}_n(\mathbb{Z})$ transformation (see Section 2.2) [2]. At the level of Laurent polynomials, if f and g are related via mutation then their classical periods agree [2, Lemma 2.8]: $\pi_f = \pi_g$. Ilten [26] has shown that if two Fano polytopes P and Q are related by mutation then the corresponding toric varieties X_P and X_Q are deformation equivalent: there exists a flat family $\mathcal{X} \to \mathbb{P}^1$ such that $\mathcal{X}_0 \cong X_P$ and $\mathcal{X}_\infty \cong X_Q$. In fact X_P and X_Q are related via a $\mathbb{Q}$-*Gorenstein (qG) deformation* [1].

Classifying Fano polygons up to mutation-equivalence thus becomes a fundamental problem. One important mutation invariant is the *singularity*

Downloaded from https://www.cambridge.org/core. IP address: 185.31.154.38, on 21 Aug 2017 at 16:48:03, subject to the Cambridge Core terms of use, available at https://www.cambridge.org/core/terms. https://doi.org/10.1017/fms.2017.10

content (see Section 3.1) [3]. This consists of a pair $(n, \mathcal{B})$, where n is an integer – the number of *primitive T-singularities* – and $\mathcal{B}$ is a *basket* – a collection of so-called *residual singularities*. A residual singularity is a cyclic quotient singularity that is rigid under qG-deformations; at the other extreme a T-singularity is a cyclic quotient singularity that admits a qG-smoothing [29]. The toric del Pezzo surface X_P is qG-deformation-equivalent to a del Pezzo surface X with singular points given by $\mathcal{B}$ and Euler number of the nonsingular locus $X \backslash \mathrm{Sing}(X)$ equal to n.

DEFINITION 1 [1]. A del Pezzo surface with cyclic quotient singularities that admits a qG-degeneration (with reduced fibres) to a normal toric del Pezzo surface is said to be of class *TG*.

Notice that not all del Pezzo surfaces can be of class TG: not every del Pezzo has $h^0(X, -K_X) > 0$, for example (see Example 5). But it is natural to conjecture the following:

CONJECTURE 1 [1, Conjecture A]. *There exists a bijective correspondence between the set of mutation-equivalence classes of Fano polygons and the set of qG-deformation-equivalence classes of locally qG-rigid class TG del Pezzo surfaces with cyclic quotient singularities.*

The main results of this paper can be seen as strong evidence in support of the conjecture above. First, an immediate consequence of Theorem 6 is:

THEOREM 1. *There are precisely ten mutation-equivalence classes of Fano polygons such that the toric del Pezzo surface X_P has only T-singularities. They are in bijective correspondence with the ten families of smooth del Pezzo surfaces.*

Second, combining the results of [14] with Theorem 9 we have:

THEOREM 2. *There are precisely* 26 *mutation-equivalence classes of Fano polygons with singularity content* $(n, \{m \times 1/3(1,1)\})$, $m \geqslant 1$. *They are in bijective correspondence with the* 26 *qG-deformation families of del Pezzo surfaces with* $m \times 1/3(1,1)$ *singular points that admit a toric degeneration.*

In Theorem 7 we prove more generally that, up to mutation, the number of Fano polygons with basket $\mathcal{B}$ is finite, and give an algorithm that outputs a finite list of Fano polygons that contains representatives for all their mutation-equivalence classes. It may happen that some of the Fano polygons produced by

Downloaded from https://www.cambridge.org/core. IP address: 185.31.154.38, on 21 Aug 2017 at 16:48:03, subject to the Cambridge Core terms of use, available at https://www.cambridge.org/core/terms. https://doi.org/10.1017/fms.2017.10

the algorithm are representatives for the same mutation-equivalence class. While there is currently no algorithm to determine whether two Fano polygons are mutation-equivalent, a useful necessary condition is provided by Lemma 3. If one accepts Conjecture 1 then Theorem 7 tells us that, for fixed basket $\mathcal{B}$, the number of qG-deformation-equivalence classes of del Pezzo surfaces of type TG with singular points $\mathcal{B}$ is finite, and gives an algorithm for classifying their toric degenerations.

1.2. An introduction from the viewpoint of cluster algebras and cluster varieties. One can obtain information about mutations of polygons using quivers and the theory of cluster algebras [16, 17]. There is a precise analogy between mutation classes of Fano polygons and the clusters of certain cluster algebras, as we now describe. Let $L \cong \mathbb{Z}^n$, and fix a skew-symmetric form $\{\cdot, \cdot\}$ on L. A *cluster* C is a transcendence basis for $\mathbb{C}(L)$, and a *seed* is a pair (B, C) where B is a basis of L. There is a notion of *mutation* of seeds, given in Definition 9 below; this depends on the form $\{\cdot, \cdot\}$. A *cluster algebra* is the algebra generated by all clusters that can be obtained from a given initial seed by mutation. To a seed (B, C) one can associate a quiver Q_B with vertex set equal to B and the number of arrows from $e_i \in B$ to $e_j \in B$ equal to $\max(\{e_i, e_j\}, 0)$. Changing the seed (B, C) by a mutation changes the quiver Q_B by a *quiver mutation* (see Definition 10). Conversely, from a quiver with vertex set B and no vertex-loops or two-cycles, one can construct a cluster algebra by setting $L = \mathbb{Z}^B$, defining $\{e_i, e_j\}$ to be the (signed) number of arrows from $e_i \in B$ to $e_j \in B$, and taking the initial seed to be (B, C), where C is the standard transcendence basis for $\mathbb{C}(L)$.

We can also associate a quiver and a cluster algebra to a Fano polygon P as follows. Suppose that the singularity content of P is $(n, \mathcal{B})$. The associated quiver Q_P has n vertices; each vertex v corresponds to a *primitive T-singularity* (Definition 3), and hence determines an edge E of P (these edges need not be distinct). The number of arrows from vertex v to vertex v' is defined to be $\max(w \wedge w', 0)$, where $\wedge$ denotes the determinant, and w and w' are the primitive inner normal vectors to the edges E and E' of P. The cluster algebra $\mathcal{A}_P$ associated to P is the cluster algebra associated to Q_P; we denote the initial seed of this cluster algebra by (B_P, C_P).

We show in Proposition 2 below that a mutation from a seed (B, C) to a seed (B', C') induces a mutation between the corresponding Fano polygons P and P'. We then show, in Proposition 3, that a mutation from a Fano polygon P to a Fano polygon P' induces a mutation between the corresponding quivers Q_P and $Q_{P'}$. These correspondences have consequences for mutation-equivalence which are not readily apparent from the polygon alone.

Downloaded from https://www.cambridge.org/core. IP address: 185.31.154.38, on 21 Aug 2017 at 16:48:03, subject to the Cambridge Core terms of use, available at https://www.cambridge.org/core/terms. https://doi.org/10.1017/fms.2017.10

EXAMPLE 1. Consider a Fano polygon $P \subset N_{\mathbb{Q}}$ containing only two primitive T-singularities, and suppose that the corresponding inner normal vectors form a basis for the dual lattice M. Then there are at most five polygons, up to $\mathrm{GL}_2(\mathbb{Z})$-equivalence, that are mutation-equivalent to P. This follows from the fact that the quiver associated to P has underlying graph A_2, and that the exchange graph of the A_2 cluster algebra is pentagonal; see Corollary 4 below.

1.3. An introduction from the viewpoint of the geometry of numbers. The relation between the lattice points in a convex body and its geometric shape and volume is a key problem in convex geometry and integer optimization. These connections have been addressed specifically for lattice polytopes, independently of their significance in toric geometry. Here we focus only on the case of interest in this paper, that of a Fano polygon. A classical result in this area is the following (these statements can be generalized and quantified, see [24]):

THEOREM 3 [31, 39]. *There are only finitely many* $\mathrm{GL}_2(\mathbb{Z})$*-equivalence classes of Fano polygons* P *with* I *interior lattice points, for each* $I \in \mathbb{Z}_{>0}$.

COROLLARY 1. *There are only a finite number of possibilities for the area and number of lattice points of a Fano polygon with* I *interior lattice points, for each* $I \in \mathbb{Z}_{>0}$.

In [2] a new equivalence relation on Fano polygons P was introduced, called *mutation-equivalence*, that is weaker than $\mathrm{GL}_2(\mathbb{Z})$-equivalence. There exist infinitely many mutation-equivalent Fano polygons that are not $\mathrm{GL}_2(\mathbb{Z})$-equivalent (see, for example, [4, Example 3.14]) and so their area and number of lattice points cannot be bounded. Mutation-equivalence does, however, preserve the Ehrhart series (and hence area) of the dual polygon $P^* \subset M_{\mathbb{Q}}$ (see Section 2.2) [2, Proposition 4].

REMARK 1. It is known that the product $\mathrm{Vol}(P) \cdot \mathrm{Vol}(P^*)$ of the (lattice normalized) area of a polygon P and of its dual polygon P^* cannot be arbitrarily small [32], however it is easy to construct families of polygons where both $\mathrm{Vol}(P)$ and $\mathrm{Vol}(P^*)$ can simultaneously become arbitrarily large. For example, $P_k := \mathrm{conv}\{(k, 1), (k, -1), (-1, 0)\}$ for $k \in \mathbb{Z}_{>0}$.

Given a Fano polygon P there exists an explicit formula for the Ehrhart series and area of the dual polygon P^* in terms of the *singularity content* of P (see Section 3.1) [3]. A consequence of this formula is that mutation-equivalent Fano polygons cannot have an arbitrarily large number of vertices [3, Lemma 3.8]; equivalently, singularity content gives an upper bound on the Picard rank of X_P under qG-deformation.

Downloaded from https://www.cambridge.org/core. IP address: 185.31.154.38, on 21 Aug 2017 at 16:48:03, subject to the Cambridge Core terms of use, available at https://www.cambridge.org/core/terms. https://doi.org/10.1017/fms.2017.10

Recall that the *height* $r_E \in \mathbb{Z}_{\geqslant 0}$ of a lattice line segment $E \subset N_{\mathbb{Q}}$ is the lattice distance of E from the origin, and the *length* of the line segment E is given by the positive integer $k = |E \cap N| - 1$. Clearly there exist unique nonnegative integers n and k_0, $0 \leqslant k_0 < r_E$, such that $k = nr_E + k_0$. Suppose that E is the edge of a Fano polygon, so that the vertices of E are primitive. As described in [3] (see also Section 3.1), one can decompose E into $n + 1$ (or n if $k_0 = 0$) lattice line segments with primitive vertices. Of these, n line segments have their length equal to their height; the cones over these line segments correspond to *primitive T-singularities*. If $k_0 \neq 0$ then there is one additional lattice line segment of length $k_0 < r_E$; the cone over this line segment corresponds to a *residual singularity*.

Although there may be several different decompositions of this form for an edge E, it turns out that the residual singularity is unique – it does not depend on the choice of decomposition. In addition, the collection of residual singularities arising from all of the edges of P, which we call the *basket* of P and denote by $\mathcal{B}$, is a mutation invariant. We say that a lattice point of P is *residual* if it lies in the strict interior of a residual cone, for some fixed choice of decomposition. The number of residual lattice points does not depend on the chosen decomposition, but only on the basket $\mathcal{B}$ of P, and is invariant under mutation. The main results of this paper can now be stated in a way analogous to the classical results above:

THEOREM 4. *There are only finitely many mutation-equivalence classes of Fano polygons P with N residual lattice points, for each $N \in \mathbb{Z}_{\geqslant 0}$.*

Proof. If there are no residual cones then the result follows from Theorem 5. In order to use Theorem 7 we only have to show that the height r_E of an edge E containing a residual cone is bounded. Let v_1 and v_2 be primitive points on E such that $\mathrm{cone}\{v_1, v_2\}$ is a residual cone. The line segment joining v_1 and v_2 has length $1 \leqslant k < r_E$. We see that the lattice triangle $\mathrm{conv}\{\mathbf{0}, v_1, v_1 + (v_2 - v_1)/k\}$ has at most $N + 3$ lattice points. Pick's formula [35] implies that its area and thus the height r_E is bounded in terms of N. □

COROLLARY 2. *There are only a finite number of possibilities for the dual area and the number of vertices of a Fano polygon with N residual lattice points, for each $N \in \mathbb{Z}_{\geqslant 0}$.*

In particular, this shows that there exist no Fano polygons with empty basket but an arbitrarily large number of vertices. Note that it can be easily seen that there exist centrally symmetric Fano polygons with an arbitrarily large number of vertices where every edge corresponds to a residual singularity.

Downloaded from https://www.cambridge.org/core. IP address: 185.31.154.38, on 21 Aug 2017 at 16:48:03, subject to the Cambridge Core terms of use, available at https://www.cambridge.org/core/terms. https://doi.org/10.1017/fms.2017.10

2. Mutation of Fano polygons

In [2, Section 3] the concept of mutation for a lattice polytope was introduced. We state it here in the simplified case of a Fano polygon $P \subset N_{\mathbb{Q}}$ and refer to [2] for the general definitions.

2.1. Mutation in N. Let $w \in M := \mathrm{Hom}(N, \mathbb{Z})$ be a primitive inner normal vector for an edge E of P, so $w : N \to \mathbb{Z}$ induces a grading on $N_{\mathbb{Q}}$ and $w(v) = -r_E$ for all $v \in E$, where r_E is the height of E. Define

$$h_{\max} := \max\{w(v) \mid v \in P\} \quad \text{and} \quad h_{\min} := -r_E = \min\{w(v) \mid v \in P\}.$$

We have that $h_{\max} > 0$ and $h_{\min} < 0$. For each $h \in \mathbb{Z}$ we define $w_h(P)$ to be the (possibly empty) convex hull of those lattice points in P at height h,

$$w_h(P) := \mathrm{conv}\{v \in P \cap N \mid w(v) = h\}.$$

By definition $w_{h_{\min}}(P) = E$ and $w_{h_{\max}}(P)$ is either a vertex or an edge of P. Let $v_E \in N$ be a primitive lattice element of N such that $w(v_E) = 0$, and define $F := \mathrm{conv}\{\mathbf{0}, v_E\}$, a line segment of unit length parallel to E at height 0. Notice that v_E, and hence F, is uniquely defined only up to sign.

DEFINITION 2. Suppose that for each negative height $h_{\min} \leqslant h < 0$ there exists a (possibly empty) lattice polytope $G_h \subset N_{\mathbb{Q}}$ satisfying

$$\{v \in \mathcal{V}(P) \mid w(v) = h\} \subseteq G_h + |h|\, F \subseteq w_h(P), \tag{1}$$

where '+' denotes the Minkowski sum, and we define $\varnothing + Q = \varnothing$ for any polytope Q. We call F a *factor* of P with respect to w, and define the *mutation* given by the primitive normal vector w, factor F, and polytopes $\{G_h\}$ to be:

$$\mathrm{mut}_w(P, F) := \mathrm{conv}\left(\bigcup_{h=h_{\min}}^{-1} G_h \cup \bigcup_{h=0}^{h_{\max}} (w_h(P) + hF)\right) \subset N_{\mathbb{Q}}.$$

Although not immediately obvious from the definition, the resulting mutation is independent of the choices of $\{G_h\}$ [2, Proposition 1]. Furthermore, up to isomorphism, mutation does not depend on the choice of v_E: we have that $\mathrm{mut}_w(P, F) \cong \mathrm{mut}_w(P, -F)$. Since we consider a polygon to be defined only up to $\mathrm{GL}_2(\mathbb{Z})$-equivalence, mutation is well defined and unique. Any mutation can be inverted by inverting the sign of w: if $Q := \mathrm{mut}_w(P, F)$ then $P = \mathrm{mut}_{-w}(Q, F)$ [2, Lemma 2]. Finally, we note that P is a Fano polygon if and only if the mutation Q is a Fano polygon [2, Proposition 2].

Downloaded from https://www.cambridge.org/core. IP address: 185.31.154.38, on 21 Aug 2017 at 16:48:03, subject to the Cambridge Core terms of use, available at https://www.cambridge.org/core/terms. https://doi.org/10.1017/fms.2017.10

We call two polygons P and $Q \subset N_{\mathbb{Q}}$ *mutation-equivalent* if there exists a finite sequence of mutations between the two polygons (considered up to $\mathrm{GL}_2(\mathbb{Z})$-equivalence). That is, if there exist polygons $P_0, P_1, \ldots, P_n$ with $P \cong P_0$, $P_{i+1} = \mathrm{mut}_{w_i}(P_i, F_i)$, and $Q \cong P_n$, for some $n \in \mathbb{Z}_{\geqslant 0}$.

REMARK 2. We remark briefly upon the three ways in which our definition above differs slightly from that in [2].

(i) First, [2] does not require that the factor F be based at the origin. The condition that $\mathbf{0} \in \mathcal{V}(F)$ is harmless, and indeed we have touched on this above when we noted that F and $-F$ give $\mathrm{GL}_2(\mathbb{Z})$-equivalent mutations: in general translation of a factor F by a lattice point $v \in w^{\perp} \cap N$, where $w^{\perp} := \{v \in N_{\mathbb{Q}} \mid w(v) = 0\}$, results in isomorphic mutations. It is reasonable to regard a factor as being defined only up to translation by elements in $w^{\perp} \cap N$, with the resulting mutation defined only up to 'shear transformations' fixing the points in $w^{\perp}$.

(ii) Second, the more general definition places no restriction on the dimension of the factor F, although the requirement that $F \subset w^{\perp}$ does mean that $\mathrm{codim}(F) \geqslant 1$. In particular it is possible to take $F = v$, where $w(v) = 0$. But observe that $v = \mathbf{0} + v$, and $\mathrm{mut}_w(\,\cdot\,, \mathbf{0})$ is the identity, hence $\mathrm{mut}_w(P, v)$ is trivial. Thus our insistence that $\dim(F) = 1$ is reasonable.

(iii) Finally, our requirement that F is of unit length is a natural simplification: in general, if the factor can be written as a Minkowski sum $F = F_1 + F_2$, where we can insist that each $F_i \subset w^{\perp}$ and $\dim(F_i) > 0$, then the mutation with factor F can be written as the composition of two mutations with factors F_1 and F_2 (with fixed w). Thus it is reasonable to assume that the factor is Minkowski-indecomposable and hence, for us, a primitive line segment.

In two dimensions, mutations are completely determined by the edges of P:

LEMMA 1. *Let E be an edge of P with primitive inner normal vector $w \in M$. Then P admits a mutation with respect to w if and only if $|E \cap N| - 1 \geqslant r_E$.*

Proof. Let $k := |E \cap N| - 1$ be the length of E. At height $h = h_{\min} = -r_E$, condition (1) becomes $E = G_{h_{\min}} + r_E F$. Hence this condition can be satisfied if and only if $k \geqslant r_E$. Suppose that $k \geqslant r_E$ and consider the cone $C := \mathrm{cone}(E)$ generated by E. At height $h_{\min} < h < 0$, $h \in \mathbb{Z}$, the line segment $C_h := \{v \in C \mid w(v) = h\} \subset N_{\mathbb{Q}}$ (with rational end points) has length $|h|\,k/r_E \geqslant |h|$. Hence $w_h(C) \subset w_h(P)$ has length at least $|h| - 1$. Suppose that there exists some $v \in \mathcal{V}(P)$ such that $w(v) = h$. Since $v \notin w_h(C)$ we conclude that $w_h(P)$ has

Downloaded from https://www.cambridge.org/core. IP address: 185.31.154.38, on 21 Aug 2017 at 16:48:03, subject to the Cambridge Core terms of use, available at https://www.cambridge.org/core/terms. https://doi.org/10.1017/fms.2017.10

length at least $|h|$. Hence condition (1) can be satisfied. If $\{v \in \mathcal{V}(P) \mid w(v) = h\} = \varnothing$ then we can simply take $G_h = \varnothing$ to satisfy condition (1). □

Lemma 1 states that the existence of a mutation of a polygon is completely determined by a purely local condition on edge length (this is not the case in higher dimensions). As a consequence, we can rephrase mutation of polygons as follows.

COROLLARY 3 (See [1]). *Choose an orientation of N and label the vertices of P by $v_1, v_2, \ldots$ counterclockwise, such that $w(v_1) = h_{\max}$ and $w(v_2) \neq h_{\max}$. Let $f \in w^{\perp} \cap N$ be a primitive lattice element. Then P admits a mutation with respect to w and the unit line segment $F = \operatorname{conv}\{\mathbf{0}, f\}$ if and only if there exists an edge $\operatorname{conv}\{v_i, v_{i+1}\}$ such that $w(v_i) = w(v_{i+1}) = h_{\min}$ and $v_{i+1} - v_i = kf$, where $k \geqslant -h_{\min}$ is a positive integer. In order to describe the mutation, we distinguish between two cases:*

(I) *P has n vertices $v_1, \ldots, v_n$ and v_1 is the unique maximum for w on P;*

(II) *P has $n+1$ vertices $v_1, \ldots, v_{n+1}$ and $w(v_1) = w(v_{n+1}) = h_{\max}$.*

Then the mutation of P with respect to w is the Fano polygon with $n+1$ vertices $v'_1, \ldots, v'_{n+1}$ given by:

Case (I)

$$v'_j = \begin{cases} v_j & \text{if } 1 \leqslant j \leqslant i; \\ v_j + w(v_j) f & \text{if } i < j \leqslant n; \\ v_1 + h_{\max} f & \text{if } j = n+1. \end{cases}$$

Case (II)

$$v'_j = \begin{cases} v_j & \text{if } 1 \leqslant j \leqslant i; \\ v_j + w(v_j) f & \text{if } i < j \leqslant n; \\ v_{n+1} + h_{\max} f & \text{if } j = n+1. \end{cases}$$

2.2. Mutation in M. Given a Fano polygon $P \subset N_{\mathbb{Q}}$ we define the *dual polygon*

$$P^* := \{u \in M_{\mathbb{Q}} \mid u(v) \geqslant -1 \text{ for all } v \in P\} \subset M_{\mathbb{Q}}.$$

In general this has rational-valued vertices and necessarily contains the origin in its strict interior. Define

$$\begin{aligned} \varphi : M_{\mathbb{Q}} &\to M_{\mathbb{Q}} \\ u &\mapsto u - u_{\min} w \quad \text{where } u_{\min} := \min\{u(v) \mid v \in F\}. \end{aligned}$$

Since $F = \operatorname{conv}\{\mathbf{0}, v_E\}$, this is equivalent to

$$\varphi(u) = \begin{cases} u & \text{if } u(v_E) \geqslant 0; \\ u - u(v_E) w & \text{if } u(v_E) < 0. \end{cases}$$

Downloaded from https://www.cambridge.org/core. IP address: 185.31.154.38, on 21 Aug 2017 at 16:48:03, subject to the Cambridge Core terms of use, available at https://www.cambridge.org/core/terms. https://doi.org/10.1017/fms.2017.10

This is a piecewise-$\mathrm{GL}_2(\mathbb{Z})$ map, partitioning $M_{\mathbb{Q}}$ into two half-spaces whose common boundary is generated by w. Crucially [2, Proposition 4 and the discussion on p. 12]:

$$\varphi(P^*) = Q^* \quad \text{where } Q := \mathrm{mut}_w(P, F).$$

An immediate consequence of this is that the area and Ehrhart series of the dual polygons are preserved under mutation:

$$\mathrm{Vol}(P^*) = \mathrm{Vol}(Q^*) \quad \text{and} \quad \mathrm{Ehr}_{P^*}(t) = \mathrm{Ehr}_{Q^*}(t).$$

Equivalently, mutation preserves the anti-canonical degree and Hilbert series of the corresponding toric varieties:

$$(-K_{X_P})^2 = (-K_{X_Q})^2 \quad \text{and} \quad \mathrm{Hilb}(X_P, -K_{X_P}) = \mathrm{Hilb}(X_Q, -K_{X_Q}).$$

EXAMPLE 2. Consider the polygon $P_{(1,1,1)} := \mathrm{conv}\{(1,1),(0,1),(-1,-2)\} \subset N_{\mathbb{Q}}$. The toric variety corresponding to $P_{(1,1,1)}$ is $\mathbb{P}^2$. Let $w = (0,-1) \in M$, so that $h_{\min} = -1$ and $h_{\max} = 2$, and set $F = \mathrm{conv}\{\mathbf{0}, (1,0)\} \subset N_{\mathbb{Q}}$. Then F is a factor of $P_{(1,1,1)}$ with respect to w, giving the mutation $P_{(1,1,2)} := \mathrm{mut}_w(P_{(1,1,1)}, F)$ with vertices $(0,1)$, $(-1,-2)$, $(1,-2)$ as depicted below. The toric variety corresponding to $P_{(1,1,2)}$ is $\mathbb{P}(1,1,4)$.

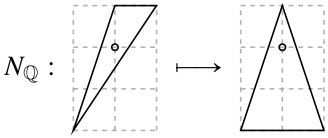

In $M_{\mathbb{Q}}$ we see the mutation as a piecewise-$\mathrm{GL}_2(\mathbb{Z})$ transformation. This acts on the left-hand half-space $\{(u_1,u_2) \in M_{\mathbb{Q}} \mid u_1 < 0\}$ via the transformation

$$(u_1,u_2) \mapsto (u_1,u_2)\begin{pmatrix} 1 & -1 \\ 0 & 1 \end{pmatrix}$$

and on the right-hand half-space via the identity.

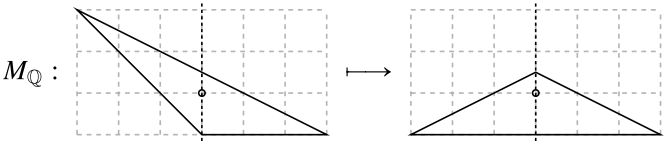

We can draw a graph of all possible mutations obtainable from $P_{(1,1,1)}$: the vertices of the graph denote $\mathrm{GL}_2(\mathbb{Z})$-equivalence classes of Fano polygons, and two

Downloaded from https://www.cambridge.org/core. IP address: 185.31.154.38, on 21 Aug 2017 at 16:48:03, subject to the Cambridge Core terms of use, available at https://www.cambridge.org/core/terms. https://doi.org/10.1017/fms.2017.10

vertices are connected by an edge if there exists a mutation between the two Fano polygons (notice that, since mutations are invertible, we can regard the edges as being undirected). We obtain a tree whose typical vertex is trivalent [4, Example 3.14]:

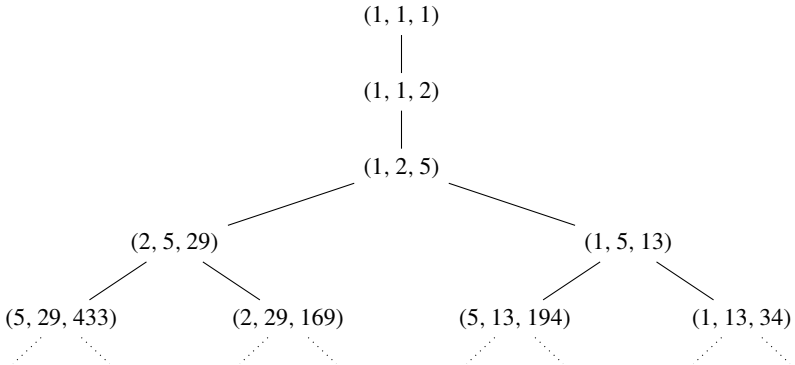

Here the vertices have been labelled with weights (a, b, c), where the polygon $P_{(a,b,c)}$ corresponds to the toric variety $\mathbb{P}(a^2, b^2, c^2)$. The triples (a, b, c) are solutions to the Markov equation

$$3xyz = x^2 + y^2 + z^2,$$

and each mutation corresponds, up to permutation of a, b, and c, to a transformation of the form $(a, b, c) \mapsto (3bc - a, b, c)$. In the theory of Markov equations these transformations are also called *mutations*. A solution (a, b, c) is called *minimal* if $a + b + c$ is minimal, and every solution can be reached via mutation from a minimal solution. Minimal solutions correspond to those triangles with $\mathrm{Vol}(P_{(a,b,c)})$ minimal. In this example $(1, 1, 1)$ is the unique minimal solution. These statements can be generalized to any mutation between triangles [4]. Hacking–Prokhorov [25] use these minimal solutions in their classification of rank-one qG-smoothable del Pezzo surfaces of class TG.

3. Invariants of Fano polygons

We wish to be able to establish whether or not two Fano polygons are mutation-equivalent. In this section we introduce two mutation invariants of a Fano polygon $P \subset N_{\mathbb{Q}}$: singularity content, discussed in Section 3.1 below, can be thought of as studying the part of P that remains untouched by mutation (the basket $\mathcal{B}$ of residual singularities); the cluster algebra $\mathcal{A}_P$, discussed in Section 3.3 below, studies the part of P that changes under mutation (the primitive T-singularities).

Downloaded from https://www.cambridge.org/core. IP address: 185.31.154.38, on 21 Aug 2017 at 16:48:03, subject to the Cambridge Core terms of use, available at https://www.cambridge.org/core/terms. https://doi.org/10.1017/fms.2017.10

Although we have no proof, it seems likely that together these two invariants completely characterize the mutation-equivalence classes. Finally, in Section 3.4 we briefly mention the connection with affine manifolds and the Gross–Seibert program [22].

3.1. Singularity content. In [3] the concept of *singularity content* for a Fano polygon was introduced. First we state the definition for a cyclic quotient singularity $1/R(a,b)$, where $\gcd\{R,a\} = \gcd\{R,b\} = 1$. (Recall that $1/R(a,b)$ denotes the germ of a quotient singularity $\mathbb{C}^2/\mu_R$, where $\varepsilon \in \mu_R$ acts via $(x,y) \mapsto (\varepsilon^a x, \varepsilon^b y)$.) Let $k, r, c \in \mathbb{Z}$ be nonnegative integers such that $k = \gcd\{R, a+b\}$, $R = kr$, and $a+b = kc$. Then r is equal to the *Gorenstein index* of the singularity, and k is called the *length* (or *width*). Thus $1/R(a,b)$ can be written in the form $1/kr(1, kc-1)$ for some $c \in \mathbb{Z}$ with $\gcd\{r,c\} = 1$.

DEFINITION 3 ($r \mid k$). A cyclic quotient singularity such that $k = nr$ for some $n \in \mathbb{Z}_{>0}$, that is, a cyclic quotient singularity of the form $1/nr^2(1, nrc-1)$, is called a *T-singularity* or a singularity of *class T*. When $n = 1$, so that the singularity is of the form $1/r^2(1, rc-1)$, we call it a *primitive T-singularity*.

DEFINITION 4 ($k < r$). A cyclic quotient singularity of the form $1/kr(1, kc-1)$ with $k < r$ is called a *residual singularity* or a singularity of *class R*.

T-singularities appear in the work of Wahl [41] and Kollár–Shepherd–Barron [29]. A cyclic quotient singularity is of class T if and only if it admits a qG-smoothing. At the opposite extreme, a singularity is of class R if and only if it is rigid under qG-deformation. More generally, consider the cyclic quotient singularity $\sigma = 1/kr(1, kc-1)$. Let $0 \leqslant k_0 < r$ and n be the unique nonnegative integers such that $k = nr + k_0$. Then either $k_0 = 0$ and σ is qG-smoothable, or $k_0 > 0$ and σ admits a qG-deformation to the residual singularity $1/k_0 r(1, k_0 c - 1)$ [1, 3]. This motivates the following definition:

DEFINITION 5 [3, Definition 2.4]. With notation as above, let $\sigma = 1/kr(1, kc-1)$ be a cyclic quotient singularity. The *residue* of σ is given by

$$\operatorname{res}(\sigma) := \begin{cases} \varnothing & \text{if } k_0 = 0; \\ \dfrac{1}{k_0 r}(1, k_0 c - 1) & \text{otherwise.} \end{cases}$$

The *singularity content* of σ is given by the pair $\operatorname{SC}(\sigma) := (n, \operatorname{res}(\sigma))$.

Downloaded from https://www.cambridge.org/core. IP address: 185.31.154.38, on 21 Aug 2017 at 16:48:03, subject to the Cambridge Core terms of use, available at https://www.cambridge.org/core/terms. https://doi.org/10.1017/fms.2017.10

EXAMPLE 3. Let $\sigma = 1/nr^2(1, nrc - 1)$ be a T-singularity. Then $\mathrm{SC}(\sigma) = (n, \varnothing)$.

Singularity content has a natural description in terms of the cone C defining the singularity. We call a two-dimensional cone $C \subset N_{\mathbb{Q}}$ a *T-cone* (respectively *primitive T-cone*) if the corresponding cyclic quotient singularity is a T-singularity (respectively primitive T-singularity), and we call C an *R-cone* if the corresponding singularity is a residual singularity. Let $C = \mathrm{cone}\{\rho_0, \rho_1\} \subset N_{\mathbb{Q}}$ be a two-dimensional cone with rays generated by the primitive lattice points ρ_0 and ρ_1 in N. The line segment $E = \mathrm{conv}\{\rho_0, \rho_1\}$ is at height r and has length $|E \cap N| - 1 = k$. Write $k = nr + k_0$. Then there exists a partial crepant subdivision of C into n cones $C_1, \ldots, C_n$ of length r and, if $k_0 \neq 0$, one cone C_0 of length $k_0 < r$. Although not immediately obvious from this description, the singularity corresponding to the R-cone C_0 is well defined and equal to $1/k_0r(1, k_0c - 1)$, where we refer to [3] for the precise definition of c. The singularities corresponding to the n primitive T-cones $C_1, \ldots, C_n$ depend upon the particular choice of subdivision: again, see [3, Proposition 2.3] for the precise statement.

DEFINITION 6. Let $P \subset N_{\mathbb{Q}}$ be a Fano polygon with edges $E_1, \ldots, E_m$, numbered cyclically, and let $\sigma_1, \ldots, \sigma_m$ be the corresponding two-dimensional cyclic quotient singularities $\sigma_i = \mathrm{cone}(E_i)$, with $\mathrm{SC}(\sigma_i) = (n_i, \mathrm{res}(\sigma_i))$. The *singularity content* of P, denoted by $\mathrm{SC}(P)$, is the pair $(n, \mathcal{B})$, where $n := \sum_{i=1}^{m} n_i$ and $\mathcal{B}$ is the cyclically ordered list $\{\mathrm{res}(\sigma_i) \mid 1 \leqslant i \leqslant m, \mathrm{res}(\sigma_i) \neq \varnothing\}$. We call $\mathcal{B}$ the *basket* of residual singularities of P.

Singularity content is a mutation invariant of P [3, Proposition 3.6]. Intuitively one can see this from Lemma 1: mutation removes a line segment of length $|h_{\min}|$ from the edge at height $h_{\min}$, changing the corresponding singularity content by $(n, \mathrm{res}(\sigma)) \mapsto (n - 1, \mathrm{res}(\sigma))$; mutation adds a line segment of length $h_{\max}$ at height $h_{\max}$, changing the singularity content by $(n', \mathrm{res}(\sigma')) \mapsto (n' + 1, \mathrm{res}(\sigma'))$. Put another way, mutation removes a primitive T-cone with Gorenstein index $-h_{\min}$ and adds a primitive T-cone with Gorenstein index $h_{\max}$, leaving the residual cones unchanged. We can rephrase Lemma 1 in terms of singularity content:

LEMMA 2. *Let E be an edge of P with primitive inner normal vector $w \in M$, and let $(n, \mathrm{res}(\sigma))$ be the singularity content of $\sigma = \mathrm{cone}(E)$. Then P admits a mutation with respect to w if and only if $n \neq 0$.*

Singularity content provides an upper bound on the maximum number of vertices of any polygon P with $\mathrm{SC}(P) = (n, \mathcal{B})$, or, equivalently, an upper bound

Downloaded from https://www.cambridge.org/core. IP address: 185.31.154.38, on 21 Aug 2017 at 16:48:03, subject to the Cambridge Core terms of use, available at https://www.cambridge.org/core/terms. https://doi.org/10.1017/fms.2017.10

on the Picard rank ρ of the corresponding toric variety X_P [3, Lemma 3.8]:

$$|\mathcal{V}(P)| \leqslant n + |\mathcal{B}|, \quad \rho \leqslant n + |\mathcal{B}| - 2. \tag{2}$$

EXAMPLE 4. Consider $P_{(1,1)} = \mathrm{conv}\{(1,0),(0,1),(-1,-3)\}$ with corresponding toric variety $\mathbb{P}(1,1,3)$. This has singularity content $(2, \{1/3(1,1)\})$, hence, by (2), any polygon Q mutation-equivalent to $P_{(1,1)}$ has three vertices. Mutations between triangles were characterized in [4]: the mutation graph is given by

$$(1,1) \text{ ——— } (1,4) \text{ ——— } (4,19) \text{ ——— } (19,91) \text{ —— } (91,436) \text{ ——— } \cdots$$

Here the vertices have been labelled by pairs $(a,b) \in \mathbb{Z}^2_{>0}$, and correspond to $\mathbb{P}(a^2,b^2,3)$ and its associated triangle. These pairs are solutions to the Diophantine equation $5xy = x^2 + y^2 + 3$. Up to exchanging a and b, a mutation of triangles corresponds to the mutation $(a,b) \mapsto (5b-a,b)$ of solutions. There is a unique minimal solution given by $(1,1)$.

As noted in Section 1.1, the toric variety X_P is qG-deformation-equivalent to a del Pezzo surface X with singular points $\mathcal{B}$ and topological Euler number of $X \backslash \mathrm{Sing}(X)$ equal to n [1, 3]. The degree and Hilbert series can be expressed purely in terms of singularity content. Recall that information about a minimal resolution of a singularity $\sigma = 1/R(1, a-1)$ is encoded in the Hirzebruch–Jung continued fraction expansion $[b_1, \ldots, b_s]$ of $R/(a-1)$; see, for example, [18]. For each $i \in \{1, \ldots, s\}$ we inductively define the positive integers α_i, β_i as follows:

$$\begin{aligned} \alpha_1 = \beta_s &= 1, \\ \alpha_i/\alpha_{i-1} &:= [b_{i-1}, \ldots, b_1], \quad 2 \leqslant i \leqslant s, \\ \beta_i/\beta_{i+1} &:= [b_{i+1}, \ldots, b_s], \quad 1 \leqslant i \leqslant s-1. \end{aligned}$$

The values $-b_i$ give the self-intersection numbers of the exceptional divisors of the minimal resolution of σ, and the values $d_i := -1 + (\alpha_i + \beta_i)/R$ give the discrepancies. The degree contribution of σ is given by:

$$A_\sigma := s + 1 - \sum_{i=1}^{s} d_i^2 b_i + 2 \sum_{i=1}^{s-1} d_i d_{i+1}.$$

The Riemann–Roch contribution Q_σ of σ can be computed in terms of Dedekind sums (see [38, Section 8]):

$$Q_\sigma = \frac{1}{1-t^R} \sum_{i=1}^{R-1} (\delta_{ai} - \delta_0)\, t^{i-1} \quad \text{where } \delta_j := \frac{1}{R} \sum_{\substack{\varepsilon \in \mu_R \\ \varepsilon \neq 1}} \frac{\varepsilon^j}{(1-\varepsilon)(1-\varepsilon^{a-1})}.$$

Downloaded from https://www.cambridge.org/core. IP address: 185.31.154.38, on 21 Aug 2017 at 16:48:03, subject to the Cambridge Core terms of use, available at https://www.cambridge.org/core/terms. https://doi.org/10.1017/fms.2017.10

PROPOSITION 1 [3, Proposition 3.3 and Corollary 3.5]. *Let $P \subset N_{\mathbb{Q}}$ be a Fano polygon with singularity content $(n, \mathcal{B})$. Let X_P be the toric variety given by the spanning fan of P. Then*

$$(-K_{X_P})^2 = 12 - n - \sum_{\sigma \in \mathcal{B}} A_\sigma$$

$$\textit{and} \quad \mathrm{Hilb}(X_P, -K_{X_P}) = \frac{1 + \big((-K_{X_P})^2 - 2\big)\,t + t^2}{(1-t)^3} + \sum_{\sigma \in \mathcal{B}} Q_\sigma .$$

The terms Q_σ can be interpreted as a periodic correction to the initial term

$$\frac{1 + ((-K_{X_P})^2 - 2)t + t^2}{(1-t)^3} = \sum_{i \geqslant 0} \left(\binom{i+1}{2} (-K_{X_P})^2 + 1 \right) t^i .$$

Set $Q_{\mathrm{num}} := (1 - t^R) Q_\sigma$. The contribution from Q_σ at degree i is equal to the coefficient of t^m in Q_{num}, where $i \equiv m \pmod R$.

EXAMPLE 5. Let $P \subset N_{\mathbb{Q}}$ be a Fano polygon with $\mathrm{SC}(P) = (n, \{m \times 1/3(1, 1)\})$, for some $n \in \mathbb{Z}_{\geqslant 0}$, $m \in \mathbb{Z}_{>0}$. Then $A_{1/3(1,1)} = 5/3$, $Q_{1/3(1,1)} = -t/3(1-t^3)$, giving

$$\mathrm{Vol}(P^*) = (-K_{X_P})^2 = 12 - n - 5m/3$$

$$\begin{aligned} \mathrm{Ehr}_{P^*}(t) &= \mathrm{Hilb}(X_P, -K_{X_P}) \\ &= \frac{1 + (11 - n - 2m)t + (12 - n - m)t^2 + (11 - n - 2m)t^3 + t^4}{(1-t^3)(1-t)^2}. \end{aligned}$$

In particular, for any $i \geqslant 0$,

$$|i\,P^* \cap M| = h^0(X_P, -i\,K_{X_P}) = \binom{i+1}{2}(-K_{X_P})^2 + 1 - \begin{cases} \dfrac{m}{3} & \text{if } i \equiv 1 \pmod 3\,; \\ 0 & \text{otherwise.} \end{cases}$$

Since $|P^* \cap M| = 13 - n - 2m \geqslant 1$ we have that $0 \leqslant n \leqslant 10$ and $1 \leqslant m \leqslant 6 - n/2$. Notice that $(5, \{4 \times 1/3(1,1)\})$, $(3, \{5 \times 1/3(1,1)\})$, and $(1, \{6 \times 1/3(1,1)\})$ give $h^0(X, -K_X) = 0$, hence there cannot exist a corresponding Fano polygon P (or toric surface X_P). They do, however, correspond to the Euler numbers and singular points of the del Pezzo surfaces $X_{4,1/3}$, $X_{5,2/3}$, and $X_{6,7/2}$, respectively, described in [14]. These three del Pezzo surfaces cannot be of class TG. It is tempting to conjecture that having $h^0(X, -K_X) = 0$ is the only obstruction to a del Pezzo surface X being of class TG.

Downloaded from https://www.cambridge.org/core. IP address: 185.31.154.38, on 21 Aug 2017 at 16:48:03, subject to the Cambridge Core terms of use, available at https://www.cambridge.org/core/terms. https://doi.org/10.1017/fms.2017.10

3.2. The sublattice Γ_P of M. There exist examples of Fano polygons that have the same singularity content, but that are not mutation-equivalent (see Example 6 below); there is additional structure in the arrangement of the primitive T-singularities that singularity content ignores.

DEFINITION 7. Let $P \subset N_{\mathbb{Q}}$ be a Fano polygon. Define Γ_P to be the sublattice of M generated by all primitive inner normal vectors w to an edge E of P with $|E \cap N| - 1 \geqslant r_E$. Let $[M : \Gamma_P]$ denote the index of this sublattice in M.

We thank one of the referees for making the following observation. After making a generic partial smoothing X of X_P the group M/Γ_P is the fundamental group of the complement U of an anti-canonical divisor in X. Indeed, U is homotopy equivalent to a torus with discs glued along representatives of homology classes defined by vanishing cycles of a (singular) torus fibration from U to a disc, and these classes are precisely the vectors $w \in M$ in Definition 7.

LEMMA 3. *Let $P \subset N_{\mathbb{Q}}$ be a Fano polygon and let $Q := \mathrm{mut}_w(P, F)$ be a mutation of P. Then $[M : \Gamma_P] = [M : \Gamma_Q]$.*

Proof. Recall from Section 2.2 that mutation acts on the element of M via the piecewise-linear map $\varphi : u \mapsto u - u_{\min} w$, where $u_{\min} := \min\{u(v_F) \mid v_F \in \mathcal{V}(F)\}$. By Lemma 1, $w \in \Gamma_P$ and φ maps Γ_P to itself. Mutations are invertible, with the inverse to $\mathrm{mut}_w(\,\cdot\,, F)$ being $\mathrm{mut}_{-w}(\,\cdot\,, F)$. Thus the index is preserved. □

EXAMPLE 6. Consider the reflexive polygons

$$R_{15} = \mathrm{conv}\{(1,0),(0,1),(-1,-1),(0,-1)\} \subset N_{\mathbb{Q}}$$
$$\text{and} \quad R_{16} = \mathrm{conv}\{(1,0),(0,1),(-1,0),(0,-1)\} \subset N_{\mathbb{Q}}.$$

The toric varieties defined via the spanning fan are the del Pezzo surfaces $\mathbb{F}_1$ and $\mathbb{P}^1 \times \mathbb{P}^1$ respectively. Both R_{15} and R_{16} have singularity content $(4, \varnothing)$. The primitive normal vectors to the edges of R_{15} generate all of M, whereas the normal vectors of the edges of R_{16} generate an index-two sublattice $\Gamma_P = \langle (1,1), (-1,1) \rangle \subset M$. Lemma 3 shows that R_{15} and R_{16} are not mutation-equivalent. We give another proof of this, using quiver mutations, in Example 7 below.

3.3. Quivers and cluster algebras. We first recall the definition of cluster algebra [16, 17], having fixed a rank-n lattice L and skew-symmetric form $\{\cdot, \cdot\}$.

DEFINITION 8. A *seed* is a pair (B, C) where B is a basis of L and C is a transcendence basis of $\mathbb{C}(L)$, referred to as a *cluster*.

Downloaded from https://www.cambridge.org/core. IP address: 185.31.154.38, on 21 Aug 2017 at 16:48:03, subject to the Cambridge Core terms of use, available at https://www.cambridge.org/core/terms. https://doi.org/10.1017/fms.2017.10

DEFINITION 9. Given a seed (B, C) with $B = \{e_1, \ldots, e_n\}$ and $C = \{x_1, \ldots, x_n\}$, the *jth mutation* of (B, C) is the seed (B', C'), where $B' = \{e'_1, \ldots, e'_n\}$ and $C' = \{x'_1, \ldots, x'_n\}$ are defined by:

$$e'_k = \begin{cases} -e_j & \text{if } k = j, \\ e_k + \max(b_{kj}, 0)e_j & \text{otherwise,} \end{cases} \quad \text{where } b_{kj} = \{e_k, e_j\},$$

$$x'_k = x_k \quad \text{if } k \neq j \quad \text{and} \quad x_j x'_j = \prod_{\substack{k \text{ such that} \\ b_{jk} > 0}} x_k^{b_{jk}} + \prod_{\substack{l \text{ such that} \\ b_{jl} < 0}} x_l^{b_{lj}}.$$

Recall from Section 1.2 that there is a quiver Q_P and a cluster algebra $\mathcal{A}_P$ associated to a Fano polygon P. Let $\mathrm{SC}(P) = (n, \mathcal{B})$ and fix a numbering of the n primitive T-cones in the spanning fan of P. The ith primitive T-cone in the spanning fan of P corresponds to a vertex v_i of Q_P, and thus corresponds to a basis element e_i in B_P, where (B_P, C_P) is the initial seed for $\mathcal{A}_P$. Let E_i denote the edge of P determined by the ith primitive T-cone; note that different primitive T-cones can determine the same edge.

PROPOSITION 2 (Mutations of seeds induce mutations of polygons). *Let $P \subset N_{\mathbb{Q}}$ be a Fano polygon with singularity content $(n, \mathcal{B})$. Denote by $w_i \in M$ the primitive inner normal vector to E_i. Consider the map $\pi\colon L \to M$ such that $\pi(e_i) = w_i$ for each i. Let (B_P, C_P) be the initial seed for $\mathcal{A}_P$, and write $B = \{e_1, \ldots, e_n\}$, $C = \{x_1, \ldots, x_n\}$. Let (B', C') be the jth mutation of (B_P, C_P), and write $B' = \{e'_1, \ldots, e'_n\}$. Then $\{\pi(e'_1), \ldots, \pi(e'_n)\}$ are the primitive inner normal vectors to the edges of P', where P' is the mutation of P determined by w_j. Furthermore, every mutation P' of P arises in this way.*

Proof. This is a straightforward calculation using mutation in M (see Section 2.2). □

There is a well-known notion of quiver mutation, going back to Bernstein–Gelfand–Ponomarev [9], Fomin–Zelevinsky [17], and others.

DEFINITION 10. Given a quiver Q and a vertex v of Q, the *mutation of Q at v* is the quiver $\mathrm{mut}(Q, v)$ obtained from Q by:

(i) adding, for each subquiver $v_1 \to v \to v_2$, an arrow from v_1 to v_2;

(ii) deleting a maximal set of disjoint two-cycles;

(iii) reversing all arrows incident to v.

Downloaded from https://www.cambridge.org/core. IP address: 185.31.154.38, on 21 Aug 2017 at 16:48:03, subject to the Cambridge Core terms of use, available at https://www.cambridge.org/core/terms. https://doi.org/10.1017/fms.2017.10

The resulting quiver is well defined up to isomorphism, regardless of the choice of two-cycles in (ii).

PROPOSITION 3 (Mutations of polygons induce mutations of quivers). *Let P be a Fano polygon, let v be a vertex of Q_P corresponding to a primitive T-cone in P, and let P' be the corresponding mutation of P. We have $Q_{P'} = \mathrm{mut}(Q_P, v)$.*

Proof. Let E denote the edge of P determined by the primitive T-cone corresponding to v, and let $w \in M$ denote the primitive inner normal vector to E. Mutation with respect to w acts on M as a piecewise-linear transformation that is the identity in one half-space, and on the other half-space is a shear transformation $u \mapsto u + (w \wedge u)w$. Thus determinants between the pairs of normal vectors change as follows.

(i) The inner normal vector w to the mutating edge E becomes $-w$, so that all arrows into v change direction.

(ii) For a pair of normal vectors in the same half-space (as defined by w), the determinant does not change.

(iii) Consider primitive T-cones with inner normal vectors in different half-spaces (as defined by w), let the corresponding vertices of Q_P be v_1 and v_2, and let the corresponding inner normal vectors in M be w_1 and w_2. Without loss of generality we may assume that $w_1 \wedge w > 0$ and $w_2 \wedge w < 0$, so that there are arrows $v_1 \to v \to v_2$ in Q_P. Under mutation, the primitive inner normal vectors change as $w_1 \mapsto w_1'$, $w_2 \mapsto w_2'$ where $w_1' = w_1$, $w_2' = w_2 + (w \wedge w_2)w$. Thus:

$$w_1' \wedge w_2' = w_1 \wedge w_2 + (w \wedge w_2)(w_1 \wedge w)$$

and so we add an arrow for each path $v_1 \to v \to v_2$. Cancelling two-cycles results in precisely the result of calculating the signed total number of arrows from v_1 to v_2.

Observing finally that if v_1, v_2 give normal vectors in the same half-space then there are no paths $v_1 \to v \to v_2$ or $v_2 \to v \to v_1$, we see that this description coincides with that of a quiver mutation. □

Propositions 2 and 3 give upper and lower bounds on the mutation graphs of Fano polygons. For example:

COROLLARY 4 (See Example 1). *If a Fano polygon P has singularity content $(2, \mathcal{B})$ and is such that the primitive inner normal vectors of the two edges*

Downloaded from https://www.cambridge.org/core. IP address: 185.31.154.38, on 21 Aug 2017 at 16:48:03, subject to the Cambridge Core terms of use, available at https://www.cambridge.org/core/terms. https://doi.org/10.1017/fms.2017.10

corresponding to the two primitive T-cones form a basis of the dual lattice M (that is, if $\Gamma_P = M$), then the mutation-equivalence class of P has at most five members.

Proof. The quiver associated to P is simply the A_2 quiver. The cluster algebra $\mathcal{A}_P$ is therefore well known (being the cluster algebra associated to the A_2 quiver) and its cluster exchange graph forms a pentagon. However, note that the *quiver* mutation graph is trivial, as the A_2 quiver mutates only to itself. Proposition 2 implies that the mutation graph of P has at most five vertices. (Proposition 3 does not give a nontrivial lower bound here: indeed polygon 7 in Figure 2 (page 40) gives an example of such a polygon P with trivial mutation graph.) □

EXAMPLE 7. For the polygons R_{15} and R_{16} considered in Example 6 above the associated quivers $Q_{R_{15}}$ and $Q_{R_{16}}$ are:

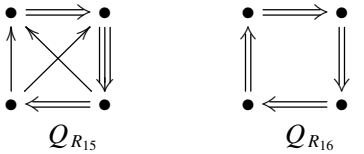

Observe that for $Q_{R_{16}}$ the number of arrows between any two vertices is even. It is easy to see that this property is preserved under mutation. Therefore, the quivers $Q_{R_{15}}$ and $Q_{R_{16}}$ are not mutation-equivalent, and so the polygons R_{15} and R_{16} are not mutation-equivalent.

REMARK 3. Following Fock–Goncharov [**16**], Gross–Hacking–Keel [**20**], and Mandel [**33**], there is a rich interplay between the theory of cluster algebras and the geometry of log Calabi–Yau surfaces.

In [**20**, Construction 5.3] a cluster structure analogous to the one defined in Section 1.2 is given. In this construction, the collection of basis vectors e_i comprising a seed is mapped to a collection of vectors w_i which are interpreted as generating elements for the rays of a fan in a two-dimensional lattice. This toric surface is then blown up at k points on each divisor D_w, where k is the number of seed vectors mapping to w, and the family of such surfaces is denoted $\mathcal{Y}$. Combining this with the construction described in Section 1.2, given a Fano polygon P we can produce a log Calabi–Yau surface by blowing up m points on the boundary of a toric surface given by the normal fan to P, where m is the singularity content of the corresponding edge of P.

Following [**20**] further, the family of surfaces $\mathcal{Y}$ obtained by this elementary birational construction agrees, up to codimension two, with the '$\mathcal{X}$-type cluster

Downloaded from https://www.cambridge.org/core. IP address: 185.31.154.38, on 21 Aug 2017 at 16:48:03, subject to the Cambridge Core terms of use, available at https://www.cambridge.org/core/terms. https://doi.org/10.1017/fms.2017.10

variety' defined in [16]. Indeed, Fock–Goncharov define a pair of (mirror-dual) varieties (the $\mathcal{X}$- and $\mathcal{A}$-type cluster varieties) directly from the data of a cluster algebra. Interpreting $\mathcal{Y}$ as a cluster variety, it is covered by *seed tori* whose transition functions are the mutations appearing in [2].

The expected mirror-duality in this context is between the $\mathcal{X}$-type cluster variety equipped with a superpotential W, and the generic smoothing of the toric variety X_P. Indeed, a mirror construction for log Calabi–Yau surfaces is described by Gross–Hacking–Keel in [21], and in [36] it is shown that, in this context, the corresponding family does indeed arise from the smoothing of the toric variety X_P.

3.4. Affine manifolds. This section sketches a more geometric approach to finding mutation invariants of polygons, based on the foundational papers of Gross–Siebert [23] and Kontsevich–Soibelman [30]. In broad terms, one wishes to generalize the fact that the dual polygon P^* is the base of a special Lagrangian torus fibration given by the moment map, by allowing more general bases and more general torus fibrations. Specifically, the base of a special Lagrangian torus fibration carries an *affine structure* [22, 30]. Deforming the torus fibration then leads to a deformation of the 'candidate base' (actually exhibiting a fibration over the deformed base is fraught with difficulty); the deformed base does not have the structure of a polygon, but rather is an *affine manifold*.

REMARK 4. While the passage from affine manifolds to algebraic geometry requires sophisticated technology from the programs of Kontsevich–Soibelman and Gross–Siebert, a construction of a *Lagrangian* fibration over this affine manifold with 'smoothed corners' was described by Symington [40].

DEFINITION 11. A two-dimensional *integral affine manifold* B is a manifold which admits a maximal atlas with transition functions in $\mathrm{GL}_2(\mathbb{Z}) \ltimes \mathbb{Z}^2$.

EXAMPLE 8. The interior of P^* is an example of an integral affine manifold, covered as it is by a single chart. The polygon P^* itself is an example of an *affine manifold with corners*.

Allowing singular fibres in the special Lagrangian torus fibration corresponds roughly to the base manifold acquiring *focus–focus singularities*. Here we say 'roughly' because, following Gross–Siebert [22], we should be considering toric *degenerations* rather than torus fibrations; see [23, 30]. The local model for such a singularity is $\mathbb{R}^2\backslash\{\mathbf{0}\}$, regarded as an affine manifold via a cover with two charts

$$U_1 = \mathbb{R}^2\backslash\mathbb{R}_{\leqslant 0} \times \{0\} \quad \text{and} \quad U_2 = \mathbb{R}^2\backslash\mathbb{R}_{\geqslant 0} \times \{0\}$$

Downloaded from https://www.cambridge.org/core. IP address: 185.31.154.38, on 21 Aug 2017 at 16:48:03, subject to the Cambridge Core terms of use, available at https://www.cambridge.org/core/terms. https://doi.org/10.1017/fms.2017.10

with the transition function

$$(x, y) \mapsto \begin{cases} (x, y) & \text{if } y > 0; \\ (x + y, y) & \text{if } y < 0. \end{cases}$$

Sliding singularities, which Kontsevich–Soibelman call *moving worms* [30], gives an affine analogue of the deformations of the varieties. In particular, allowing singularities to collide with boundary points of the affine manifold creates corners and provides an analogue for the toric qG-degenerations of the surface. This process, and its lifting via the Gross–Siebert program to construct the corresponding degeneration of algebraic varieties, are described in [36].

Given the dual polygon P^*, the set of singularities that we can introduce is in natural bijection with the primitive T-cones appearing in the singularity content of P. Consider the following process. Take a primitive T-cone σ of P, and introduce the corresponding singularity into the interior of P^*, partially smoothing that corner and forming an affine manifold B. Now slide this singularity along the monodromy-invariant line, all the way to the opposite of B, and so forming a polygon P'^* with dual polygon P'.

LEMMA 4. *P' is equal to the mutation of P defined by the primitive T-cone σ.*

Proof. Mutation induces a piecewise-linear transformation on the dual polygon. In fact this corresponds exactly to the transition function between the two charts defining B. As the singularity approaches a corner, one of the charts covers all but a line segment with vanishing length, hence the polygons are related by the piecewise-linear transition function applied to the entire polygon. □

Given a polygon P^* one can introduce a maximal set of singularities and thus form an affine manifold B. Regarding two affine manifolds which differ by moving singularities along monodromy-invariant lines as equivalent, we see that every polygon in the same mutation class is equivalent as an affine manifold. This gives a mutation invariant — the affine manifold B — which we can use to distinguish minimal polygons. Specifically, we can compare the respective *monodromy representations*. Since the transition functions of B are in $\mathrm{GL}_2(\mathbb{Z})$ we can define parallel transport of integral vector fields. Fixing a basepoint in B, parallel transport around loops gives a representation $\pi_1(B) \to \mathrm{SL}_2(\mathbb{Z})$. Properties of this representation may be used to distinguish different mutation classes of polygons. For example, in the cases considered in Example 6, one monodromy representation is surjective and the other is not.

Downloaded from https://www.cambridge.org/core. IP address: 185.31.154.38, on 21 Aug 2017 at 16:48:03, subject to the Cambridge Core terms of use, available at https://www.cambridge.org/core/terms. https://doi.org/10.1017/fms.2017.10

4. Minimal Fano polygons

Given a polygon $P \subset N_{\mathbb{Q}}$ we want to find a preferred representative in the mutation-equivalence class of P. Let ∂P denote the boundary of P and let $P^\circ := P \backslash \partial P$ denote the strict interior of P. We introduce the following definition:

DEFINITION 12. We call a Fano polygon $P \subset N_{\mathbb{Q}}$ *minimal* if for every mutation $Q := \mathrm{mut}_w(P, F)$ we have that $|\partial P \cap N| \leqslant |\partial Q \cap N|$.

Minimality is a local property of the mutation graph. It is certainly possible for there to exist more than one minimal polygon in a given mutation-equivalence class (see Example 9 below); however, the number is finite. This is shown in Theorem 5 in the case when $\mathcal{B} = \varnothing$, and in Theorem 7 when $\mathcal{B} \neq \varnothing$. Given a polygon $P \subset N_{\mathbb{Q}}$ one can easily construct a mutation-equivalent minimal polygon. Set $P_0 := P$ and recursively define P_{i+1} as follows. Let $\Gamma_i := \{P_i\} \cup \{\mathrm{mut}_w(P_i, F) \mid \text{ for all possible } w \in M\}$ where, as usual, we regard a polygon as being defined only up to $\mathrm{GL}_2(\mathbb{Z})$-equivalence. Pick $P_{i+1} \in \Gamma_i$ such that $|\partial P_{i+1} \cap N| = \min\{|\partial Q \cap N| \mid Q \in \Gamma_i\}$. If $|\partial P_i \cap N| = |\partial P_{i+1} \cap N|$ we stop, and P_i is minimal. Notice that this process must terminate in a finite number of steps.

LEMMA 5 (Characterization of minimality). *Let $P \subset N_{\mathbb{Q}}$ be a Fano polygon. The following are equivalent:*

(i) *P is minimal;*

(ii) *$|\partial P \cap N| \leqslant |\partial Q \cap N|$ for every mutation $Q := \mathrm{mut}_w(P, F)$;*

(iii) *$|P^\circ \cap N| \leqslant |Q^\circ \cap N|$ for every mutation $Q := \mathrm{mut}_w(P, F)$;*

(iv) *$\mathrm{Vol}(P) \leqslant \mathrm{Vol}(Q)$ for every mutation $Q := \mathrm{mut}_w(P, F)$;*

(v) *$r_1 + \cdots + r_n \leqslant s_1 + \cdots + s_n$ for every mutation $Q := \mathrm{mut}_w(P, F)$, where the r_i (respectively s_i) are the Gorenstein indices of the primitive T-cones associated with P (respectively Q).*

Proof. Let C be an arbitrary cone (not necessarily a T-cone) corresponding to the cyclic quotient singularity $1/R(a, b)$. Let $\rho_1, \rho_2 \in N$ be the primitive lattice vectors generating the rays of C. Recall that $k = \gcd\{R, a + b\}$ is the length of the line segment $\rho_1\rho_2$, and that the Gorenstein index $r = R/\gcd\{R, a + b\}$ is the height of $\rho_1\rho_2$. Set $D := \mathrm{conv}\{\rho_1, \rho_2, \mathbf{0}\}$. Since $R = k + 2\,|D^\circ \cap N|$ we have that:

$$|D^\circ \cap N| = \frac{R - k}{2} = \frac{k(r - 1)}{2}.$$

If C is a primitive T-cone then $r = k$.

Downloaded from https://www.cambridge.org/core. IP address: 185.31.154.38, on 21 Aug 2017 at 16:48:03, subject to the Cambridge Core terms of use, available at https://www.cambridge.org/core/terms. https://doi.org/10.1017/fms.2017.10

Let P have singularity content $(n, \mathcal{B})$, and let $r_1, \ldots, r_n$ be the Gorenstein indices of the primitive T-cones. Then the number of boundary points is

$$|\partial P \cap N| = \sum_{i=1}^{n} r_i + \sum_{\mathcal{B}} (|\partial D \cap N| - 1), \tag{3}$$

where $\sum_{\mathcal{B}}(|\partial D \cap N| - 1)$ is the contribution arising from the basket $\mathcal{B}$, and the number of interior points is given by

$$|P^\circ \cap N| = 1 + \frac{1}{2}\sum_{i=1}^{n} r_i(r_i - 1) + \sum_{\mathcal{B}} |D^\circ \cap N|, \tag{4}$$

where $\sum_{\mathcal{B}} |D^\circ \cap N|$ is the contribution arising from the basket $\mathcal{B}$. Notice that the values of both $\sum_{\mathcal{B}}(|\partial D \cap N| - 1)$ and $\sum_{\mathcal{B}} |D^\circ \cap N|$ are fixed under mutation. By applying Pick's formula we obtain

$$\mathrm{Vol}(P) = |\partial P \cap N| + 2\,|P^\circ \cap N| - 2 = \sum_{i=1}^{n} r_i^2 + B \tag{5}$$

where $B := \sum_{\mathcal{B}}(|\partial D \cap N| - 1) + 2\sum_{\mathcal{B}} |D^\circ \cap N|$ is a constant under mutation. Mutation can change the value of only one r_i at a time, hence equations (3), (4), and (5) are all locally minimal with respect to mutation if and only if $r_1 + \cdots + r_n$ is locally minimal with respect to mutation. □

REMARK 5. Recall that mutations between Fano triangles are characterized in terms of solutions to a Diophantine equation [4]. Every solution can be obtained from a minimal solution – a solution $(a, b, c) \in \mathbb{Z}^3_{>0}$ whose sum $a + b + c$ is minimal – and a minimal solution corresponds to a triangle with smallest area [4, Lemma 3.16]. By Lemma 5(iv) we see that the notion of minimality introduced in Definition 12 above can be viewed as a generalization of the concept of minimal solution.

EXAMPLE 9. Any reflexive polygon P has $|P^\circ \cap N| = 1$, and so is minimal by Lemma 5(iii). In particular this gives us examples of mutation-equivalent polygons $P_1 \ncong P_2$, both of which are minimal. For example, one could take $P_1 = \mathrm{conv}\{(\pm 1, 0), (0, \pm 1)\}$ and $P_2 = \mathrm{conv}\{(1, 0), (0, 1), (-1, -2)\}$ (the polygons associated with $\mathbb{P}^1 \times \mathbb{P}^1$ and $\mathbb{P}(1, 1, 2)$, respectively).

An immediate consequence of Lemma 5(v) is the following:

COROLLARY 5. *Let $P \subset N_{\mathbb{Q}}$ be a Fano polygon. For each edge E of P let $w_E \in M$ denote the corresponding primitive inner normal vector and let k_E denote the length. P is minimal if and only if $|h_{\min}| \leqslant h_{\max}$ for each w_E such that $k_E \geqslant |h_{\min}|$.*

Downloaded from https://www.cambridge.org/core. IP address: 185.31.154.38, on 21 Aug 2017 at 16:48:03, subject to the Cambridge Core terms of use, available at https://www.cambridge.org/core/terms. https://doi.org/10.1017/fms.2017.10

EXAMPLE 10. Any centrally symmetric polygon (that is, any polygon P satisfying $v \in P$ if and only if $-v \in P$) is minimal: for any primitive inner normal vector $w \in M$, $|h_{\min}| = h_{\max}$.

COROLLARY 6. *Let $P := \mathrm{conv}\{v_0, v_1, v_2\}$ be a Fano triangle with residual basket $\mathcal{B} = \varnothing$. Then P is minimal if and only if $v_0 + v_1 + v_2 \in P$.*

Proof. Set $\overline{v} := v_0 + v_1 + v_2 \in N$. Let E be an edge of P and let $w \in M$ be the corresponding primitive inner normal vector. Then $w(\overline{v}) = w(v_0) + w(v_1) + w(v_2) = 2h_{\min} + h_{\max}$, and $|h_{\min}| \leqslant h_{\max}$ if and only if $\overline{v}$ lies in the half-space $H_E := \{v \in N_{\mathbb{Q}} \mid w(v) \geqslant h_{\min}\}$. By Corollary 5 we have that P is minimal if and only if $\overline{v} \in \bigcap H_E$, where the intersection is taken over all edges E of P. The result follows. □

5. Minimal Fano polygons with only T-singularities

In Theorem 5 below we classify all minimal Fano polygons with residual basket $\mathcal{B} = \varnothing$. Conjecture 1 tells us that the mutation-equivalence classes should correspond to the ten qG-deformation classes of smooth del Pezzo surfaces, and in Theorem 6 we find that this is indeed what happens. In particular, in the case when X_P is a rank-one toric del Pezzo surface with only T-singularities we recover the results of Hacking–Prokhorov [**25**, Theorem 4.1]. Perling has also studied these surfaces from the viewpoint of mutations of exceptional collections [**34**].

DEFINITION 13. Let $P \subset N_{\mathbb{Q}}$ be a Fano polygon with vertex set denoted by $\mathcal{V}(P)$ and edge set denoted by $\mathcal{F}(P)$. For each edge $E \in \mathcal{F}(P)$ of P the unique primitive lattice point in the dual lattice $M := \mathrm{Hom}(N, \mathbb{Z})$ defining an inner normal of E is denoted by w_E. The positive integer $r_E := -w_E(E)$ (that is, the height of E above the origin $\mathbf{0}$) is equal to the Gorenstein index of the singularity associated with cone(E). We call r_E the *Gorenstein index* (or *local index*) of E. The *maximum Gorenstein index* (also called the *maximum local index*) is the maximum Gorenstein index of all edges of P:

$$m_P := \max\{r_E \mid E \in \mathcal{F}(P)\}.$$

The *Gorenstein index* r_P of a Fano polygon P is the least common multiple of the Gorenstein indices:

$$r_P := \mathrm{lcm}\{r_E \mid E \in \mathcal{F}(P)\}.$$

Equivalently, r_P is equal to the smallest positive integer ℓ such that ℓP^* is a lattice polygon. In terms of the toric variety X_P, r_P is equal to the smallest positive integer ℓ such that $-\ell K_{X_P}$ is Cartier.

Downloaded from https://www.cambridge.org/core. IP address: 185.31.154.38, on 21 Aug 2017 at 16:48:03, subject to the Cambridge Core terms of use, available at https://www.cambridge.org/core/terms. https://doi.org/10.1017/fms.2017.10

LEMMA 6. *Let* $P = \operatorname{conv}\{v_0, v_1, v_2\} \subset N_{\mathbb{Q}}$ *be a Fano triangle, and let* $(\lambda_0, \lambda_1, \lambda_2) \in \mathbb{Z}^3_{>0}$ *be such that* $\lambda_0 v_0 + \lambda_1 v_1 + \lambda_2 v_2 = \mathbf{0}$. *Then:*

$$\operatorname{Vol}(P) \cdot \operatorname{Vol}(P^*) = \frac{(\lambda_0 + \lambda_1 + \lambda_2)^3}{\lambda_0 \lambda_1 \lambda_2}.$$

Proof. We give a toric proof; for a combinatorial argument, see [6, Proposition 6.2]. We can assume that the weights $(\lambda_0, \lambda_1, \lambda_2)$ are coprime and, since P is a Fano polygon, this implies that the weights are pairwise coprime. Recall [27] that the Fano triangle P corresponds to some fake weighted projective space $X_P = \mathbb{P}(\lambda_0, \lambda_1, \lambda_2)/G$, where $G = N/N'$ is the quotient of N by the sublattice $N' = v_0 \cdot \mathbb{Z} + v_1 \cdot \mathbb{Z} + v_2 \cdot \mathbb{Z}$ generated by the vertices of P. The order $|G|$, or equivalently the index $[N : N']$ of the sublattice N', is called the *multiplicity* of P, and denoted by $\operatorname{mult}(P)$. Let $Q \subset N_{\mathbb{Q}}$ be the Fano triangle associated with weighted projective space $X_Q = \mathbb{P}(\lambda_0, \lambda_1, \lambda_2)$. Then

$$\operatorname{Vol}(Q) = \lambda_0 + \lambda_1 + \lambda_2 \quad \text{and} \quad \operatorname{Vol}(Q^*) = \frac{(\lambda_0 + \lambda_1 + \lambda_2)^2}{\lambda_0 \lambda_1 \lambda_2},$$

where the second value is simply the degree $(-K_{X_Q})^2$ of the weighted projective space X_Q. But Q is $\mathrm{GL}_2(\mathbb{Z})$-equivalent to the restriction of P to N'. Hence $\operatorname{Vol}(P) = \operatorname{mult}(P) \cdot \operatorname{Vol}(Q)$ and:

$$\operatorname{Vol}(P^*) = \frac{1}{\operatorname{mult}(P)} \cdot \operatorname{Vol}(Q^*) = \frac{(\lambda_0 + \lambda_1 + \lambda_2)^3}{\lambda_0 \lambda_1 \lambda_2} \cdot \frac{1}{\operatorname{Vol}(P)}. \qquad \square$$

LEMMA 7 [28, Lemma 2.1]. *Let* $P \subset N_{\mathbb{Q}}$ *be a Fano polygon and let* E *be an edge with Gorenstein index equal to the maximum Gorenstein index of* P, $r_E = m_P$. *Assume that there exists a nonvertex lattice point* $v \in \operatorname{cone}(E)$ *with* $w_E(v) = -1$. *For every lattice point* $v' \in P \cap N \setminus E$ *we have that* $v + v' \in P \cap N$. *In particular, if* E' *is an edge of* P *that is not parallel to* v, *then* $|E' \cap N| \leqslant |E \cap N|$.

THEOREM 5. *Let* $P \subset N_{\mathbb{Q}}$ *be a minimal Fano polygon with residual basket* $\mathcal{B} = \varnothing$. *Then, up to* $\mathrm{GL}_2(\mathbb{Z})$*-equivalence,* P *is one of the following* 35 *polygons:*

(i) *the five reflexive triangles* $R_1, \ldots, R_5$ *in Table* 1;

(ii) *the eleven reflexive polygons* $R_6, \ldots, R_{16}$ *in Table* 2;

(iii) *the nine nonreflexive triangles* $T_1, \ldots, T_9$ *in Table* 1;

(iv) *the ten nonreflexive polygons* $P_1, \ldots, P_{10}$ *in Table* 2.

Downloaded from https://www.cambridge.org/core. IP address: 185.31.154.38, on 21 Aug 2017 at 16:48:03, subject to the Cambridge Core terms of use, available at https://www.cambridge.org/core/terms. https://doi.org/10.1017/fms.2017.10

Downloaded from https://www.cambridge.org/core. IP address: 185.31.154.38, on 21 Aug 2017 at 16:48:03, subject to the Cambridge Core terms of use, available at https://www.cambridge.org/core/terms. https://doi.org/10.1017/fms.2017.10

Table 1. The minimal Fano triangles $P \subset N_{\mathbb{Q}}$ with singularity content $(n, \varnothing)$, vertices $\mathcal{V}(P)$, maximum Gorenstein index m_P, and weights $(\lambda_0, \lambda_1, \lambda_2)$, up to the action of $\mathrm{GL}_2(\mathbb{Z})$. The corresponding toric varieties X_P and degrees $(-K_{X_P})^2 = 12 - n$ are also given. Those P marked with $\star$ are chosen as the representative polygon in the mutation-equivalence class, and are depicted in Figure 1 (page 32).

P	$\mathcal{V}(P)$	λ_0	λ_1	λ_2	X_P	m_P	n	$(-K_{X_P})^2$
$\star R_1$	$(1,0),(0,1),(-1,-1)$	1	1	1	$\mathbb{P}^2$	1	3	9
$\star R_2$	$(1,1),(-2,1),(1,-2)$	1	1	1	$\mathbb{P}^2/(\mathbb{Z}/3)$	1	9	3
T_1	$(1,3),(-2,3),(1,-6)$	1	1	1	$\mathbb{P}^2/(\mathbb{Z}/9)$	3	11	1
R_3	$(1,1),(-1,1),(0,-1)$	1	1	2	$\mathbb{P}(1,1,2)$	1	4	8
R_4	$(1,1),(-1,1),(1,-3)$	1	1	2	$\mathbb{P}(1,1,2)/(\mathbb{Z}/2)$	1	8	4
T_2	$(1,2),(-1,2),(1,-6)$	1	1	2	$\mathbb{P}(1,1,2)/(\mathbb{Z}/4)$	2	10	2
$\star T_3$	$(3,2),(-1,2),(-1,-2)$	1	1	2	$\mathbb{P}(1,1,2)/(\mathbb{Z}/4)$	2	10	2
T_4	$(1,4),(-3,4),(1,-4)$	1	1	2	$\mathbb{P}(1,1,2)/(\mathbb{Z}/8)$	4	11	1
R_5	$(1,1),(-1,1),(1,-2)$	1	2	3	$\mathbb{P}(1,2,3)$	1	6	6
T_5	$(1,2),(-1,2),(1,-4)$	1	2	3	$\mathbb{P}(1,2,3)/(\mathbb{Z}/2)$	2	9	3
T_6	$(1,3),(-2,3),(1,-3)$	1	2	3	$\mathbb{P}(1,2,3)/(\mathbb{Z}/3)$	3	10	2
$\star T_7$	$(5,3),(-1,3),(-1,-3)$	1	2	3	$\mathbb{P}(1,2,3)/(\mathbb{Z}/6)$	3	11	1
T_8	$(1,2),(-1,2),(1,-3)$	1	4	5	$\mathbb{P}(1,4,5)$	2	7	5
T_9	$(2,5),(-3,5),(2,-5)$	1	4	5	$\mathbb{P}(1,4,5)/(\mathbb{Z}/5)$	5	11	1

Table 2. The minimal Fano m-gons, $m \geqslant 4$, $P \subset N_{\mathbb{Q}}$ with singularity content $(n, \varnothing)$, vertices $\mathcal{V}(P)$, and maximum Gorenstein index m_P, up to the action of $\mathrm{GL}_2(\mathbb{Z})$. The degrees $(-K_{X_P})^2 = 12 - n$ of the corresponding toric varieties are also given. Those P marked with $\star$ are chosen as the representative polygon in the mutation-equivalence class, and are depicted in Figure 1 (page 32).

P	$\mathcal{V}(P)$	m_P	n	$(-K_{X_P})^2$
P_1	$(1,2),(-1,2),(-1,-2),(1,-2)$	2	10	2
P_2	$(1,2),(-1,2),(-1,-1),(1,-3)$	2	10	2
P_3	$(1,2),(-1,2),(-1,0),(1,-4)$	2	10	2
P_4	$(1,2),(-1,2),(-1,1),(1,-5)$	2	10	2
P_5	$(1,2),(-1,2),(-1,0),(1,-2)$	2	9	3
P_6	$(1,2),(-1,2),(-1,1),(1,-3)$	2	9	3
R_6	$(1,1),(-1,1),(-1,0),(1,-2)$	1	8	4
$\star R_7$	$(1,1),(-1,1),(-1,-1),(1,-1)$	1	8	4
P_7	$(1,2),(-1,2),(0,-1),(1,-3)$	2	8	4
P_8	$(1,2),(-1,2),(-1,1),(0,-1),(1,-2)$	2	8	4
R_8	$(1,1),(-1,1),(0,-1),(1,-2)$	1	7	5
P_9	$(1,2),(-1,2),(-1,1),(1,-2)$	2	7	5
P_{10}	$(1,2),(-1,2),(0,-1),(1,-2)$	2	7	5
$\star R_9$	$(1,1),(-1,1),(-1,0),(0,-1),(1,-1)$	1	7	5
R_{10}	$(1,1),(-1,1),(-1,0),(1,-1)$	1	6	6
R_{11}	$(1,0),(1,1),(-1,1),(-1,0),(0,-1)$	1	6	6
$\star R_{12}$	$(1,0),(1,1),(0,1),(-1,0),(-1,-1),(0,-1)$	1	6	6
R_{13}	$(1,0),(1,1),(-1,1),(0,-1)$	1	5	7
$\star R_{14}$	$(1,0),(1,1),(0,1),(-1,-1),(0,-1)$	1	5	7
$\star R_{15}$	$(1,0),(0,1),(-1,-1),(0,-1)$	1	4	8
$\star R_{16}$	$(1,0),(0,1),(-1,0),(0,-1)$	1	4	8

Proof. We consider the cases when P is reflexive, that is $m_P = 1$, and when P is not reflexive, that is $m_P > 1$, separately.

$m_P = 1$: Every reflexive polygon is minimal since $|P^\circ \cap N| = 1$. The classification of the reflexive polygons is well known: up to $\mathrm{GL}_2(\mathbb{Z})$-equivalence

Downloaded from https://www.cambridge.org/core. IP address: 185.31.154.38, on 21 Aug 2017 at 16:48:03, subject to the Cambridge Core terms of use, available at https://www.cambridge.org/core/terms. https://doi.org/10.1017/fms.2017.10

there are sixteen polygons [7, 37], of which five are triangles. This proves (i) and (ii).

$\underline{m_P > 1}$: Let $E \in \mathcal{F}(P)$ be an edge of maximum Gorenstein index $r_E = m_P > 1$. By assumption the length of E is some multiple $k \in \mathbb{Z}_{>0}$ of r_E, that is, $|E \cap N| = kr_E + 1$. Since the cone $C = \mathrm{cone}(E)$ is a union of k primitive T-cones, each of which contains exactly one point at height -1 with respect to w_E, there exist k distinct points $v_1, \ldots, v_k \in C^\circ \cap N$ such that $w_E(v_i) = -1$. After suitable change of basis we can insist that $E = \mathrm{conv}\{(-a, r_E), (b, r_E)\}$ where $a, b > 0$, $a < r_E$, and $a + b = kr_E$. Hence the point $((i-1)r_E, r_E)$ lies in the strict interior of E and so, after possible reordering, $v_i = (i-1, 1)$, for each $i = 1, \ldots, k$.

Let $v \in \mathcal{V}(P)$ be a vertex of P such that $w_E(v) = \max\{w_E(v') \mid v' \in P\} = h_{\max}$. Since P is minimal by assumption, we have that $w_E(v) \geqslant r_E = |h_{\min}|$ (Corollary 5). By Lemma 7 we have that v is contained in the strip $E - v_1 \cdot \mathbb{Z}_{>0}$. Hence we can write $v = (\alpha, -\beta)$ for some $\beta \geqslant r_E$ and $-a \leqslant \alpha \leqslant b$. If $k > 1$ then we have $v \in E - v_k \cdot \mathbb{Z}_{>0}$ and so

$$-a \leqslant \alpha \leqslant b - (k-1)(r_E + \beta) \leqslant b - 2(k-1)r_E = -a - (k-2)r_E. \qquad (6)$$

We conclude that $k \leqslant 2$.

$\underline{k = 2}$: Let us first consider the case when $k = 2$. By (6) P is a triangle given by

$$P = \mathrm{conv}\{(-a, r_E), (-a + 2r_E, r_E), (-a, -r_E)\},$$
$$\text{where } 0 < a < r_E, \gcd\{a, r_E\} = 1.$$

Let $E' \in \mathcal{F}(P)$ be the edge with vertices $(-a, r_E)$ and $(-a, -r_E)$. Since the corresponding cone is of class T, we have that $a \mid 2r_E$, and so $a = 1$ or 2. Analogously, by considering the edge with vertices $(-a, -r_E)$ and $(2r_E - a, r_E)$ of length $2r_E$ and Gorenstein index $r_E - a$, we see $r_E - a \mid 2r_E$. This leads to $(r_E, a) \in \{(2, 1), (3, 1), (3, 2), (4, 2), (6, 2)\}$. The first possibility gives the triangle T_3 in Table 1, the second and third possibilities define the triangle T_7, and the final two possibilities are excluded because of $\gcd\{a, r_E\} = 1$.

$\underline{k = 1}$: We now consider the case when $k = 1$. This is subdivided into two cases depending on whether or not there exists an edge $E' \in \mathcal{F}(P)$ parallel to E.

$\underline{\text{Edge } E' \text{ parallel to } E}$: Let us assume that there exists a second point of P at height $w_E(v)$; that is, that there exists an edge $E' \in \mathcal{F}(P)$ such that $w_E(E') = w_E(v)$, so that E and E' are parallel. By minimality we see that $r_{E'} = r_E$, and by Lemma 7 we have that $|E' \cap N| \leqslant |E \cap N| = r_E + 1$. Recalling that $\mathrm{cone}(E')$ is a T-cone, and hence $r_{E'} \mid |E' \cap N| - 1$, we see that P is a rectangle:

$$P = \mathrm{conv}\{(-a, r_E), (-a + r_E, r_E), (-a, -r_E), (-a + r_E, -r_E)\}.$$

Downloaded from https://www.cambridge.org/core. IP address: 185.31.154.38, on 21 Aug 2017 at 16:48:03, subject to the Cambridge Core terms of use, available at https://www.cambridge.org/core/terms. https://doi.org/10.1017/fms.2017.10

Since P is minimal we have that $2a = r_E$ and, by primitivity of the vertices, $a = 1$, $r_E = 2$, giving P_1 in Table 2.

No edge parallel to E: We are now in the situation where v is the unique vertex satisfying $w_E(v) = \max\{w_E(v') \mid v' \in P\}$. We subdivide this into two cases depending on whether one of the edges $E' \in \mathcal{F}(P)$ with vertex v is vertical.

E' not vertical: Let us assume that there is no vertical edge adjacent to $v = (\alpha, -\beta)$. We consider the case $\alpha \geqslant 0$ (the case $\alpha < 0$ being similar). By our assumption, we can choose an edge E' adjacent to v with $w_{E'} = (-\gamma, \delta) \in M$, where $\gamma, \delta \geqslant 1$. We have that $r_E \geqslant -w_{E'}(v) = \gamma\alpha + \delta\beta \geqslant \alpha + \beta \geqslant \beta \geqslant r_E$. Hence $(\alpha, -\beta) = (0, -r_E)$, $w_{E'} = (-\gamma, 1)$, and $r_{E'} = r_E = m_P$. Exchanging the roles of E and E' we have that E' is of length either $2r_E$, in which case we are in the case $k = 2$ above, or of length r_E, in which case $(r_E, (\gamma - 1)r_E)$ is a vertex of P. This is a contradiction, since as $r_E > b$, this vertex is not contained in the strip $E - v_1 \cdot \mathbb{Z}_{>0}$.

E' vertical: The majority of cases arise when v is contained in a vertical edge $E' \in \mathcal{F}(P)$. This edge necessarily contains one of the two vertices of E, and without loss of generality (since $a + b = r_E$) we may assume that $E' = \mathrm{conv}\{v, (b, r_E)\}$. Hence $v = (b, r_E - jb)$ for some $j \in \mathbb{Z}_{>0}$. Minimality forces $r_E - jb \leqslant -r_E$, so that

$$jb \geqslant 2r_E. \tag{7}$$

Moreover, minimality implies

$$2b \leqslant r_E. \tag{8}$$

In particular we see that $j \geqslant 4$.

$j = 4$: The case when $j = 4$ is different from the cases when $j \geqslant 5$, and we deal with it now. Equations (7) and (8) gives that $2b = r_E$, and so by primitivity we have that $r_E = 2$ and $b = 1$. Hence P is contained in the rectangle $[-1, 1] \times [-2, 2]$. Notice that the requirement that $\mathbf{0} \in P^\circ$ means that P cannot be a triangle. We find P_5, P_8, P_9, and P_{10} in Table 2.

$j \geqslant 5$: Consider the triangle

$$T := \mathrm{conv}\{(b - r_E, r_E), (b, r_E), (b, r_E - jb)\}.$$

By (7) $-r_E \geqslant r_E - jb$, so the point $(b, -r_E)$ is in T. The midpoint of $(b, -r_E)$ and $(b - r_E, r_E)$ is $(b - r_E/2, 0)$. Equation (8) implies $b - r_E/2 \leqslant 0$. If $b - r_E/2 < 0$ then $\mathbf{0} \in T^\circ$. If $b - r_E/2 = 0$ then $j \geqslant 5$ implies that $(b, -r_E)$ is not equal to the vertex $(b, r_E - jb)$, so $\mathbf{0} = (b - r_E/2, 0) \in T^\circ$ again.

This shows that T is a Fano triangle. We have that $\mathrm{Vol}(T) = jbr_E$. Moreover, one can check that

$$(jb^2, jbr_E - jb^2 - r_E^2, r_E^2) \in \mathbb{Z}^3_{>0}$$

Downloaded from https://www.cambridge.org/core. IP address: 185.31.154.38, on 21 Aug 2017 at 16:48:03, subject to the Cambridge Core terms of use, available at https://www.cambridge.org/core/terms. https://doi.org/10.1017/fms.2017.10

satisfy the conditions of Lemma 6. Hence

$$\mathrm{Vol}(T^*) = \frac{j}{jbr_E - jb^2 - r_E^2}.$$

By Proposition 1 (note $\mathrm{Vol}(P^*) = (-K_{X_P})^2$ and $\mathcal{B} = \varnothing$), $\mathrm{Vol}(P^*) \in \mathbb{Z}_{>0}$, and so $1 \leqslant \mathrm{Vol}(P^*) \leqslant \mathrm{Vol}(T^*)$. Let $b = r_E q$, where $2/j \leqslant q \leqslant 1/2$, by (7) and (8), so that the lower bound on $\mathrm{Vol}(T^*)$ gives:

$$r_E^2(-jq^2 + jq - 1) \leqslant j. \tag{9}$$

The quadratic in q on the left-hand side of (9) is strictly positive in the range $2/j \leqslant q \leqslant 1/2$ and obtains its minimum value when $q = 2/j$. Hence (9) gives:

$$r_E^2 \leqslant \frac{j^2}{j-4}. \tag{10}$$

Recall from Proposition 1 that $\mathrm{Vol}(P^*) = 12 - n \geqslant 1$, where n is the total number of primitive T-cones spanned by the edges of P; equivalently,

$$n = \sum_{F \in \mathcal{F}(P)} \frac{|F \cap N| - 1}{r_F}.$$

Since P must have at least three edges, each of which corresponds to a T-cone, and by construction we have that the top edge decomposes into a single primitive T-cone, and that the right-hand vertical edge E' decomposes into $j \geqslant 5$ primitive T-cones, we conclude that $j \in \{5, \ldots, 9\}$. From the inequalities (7), (8), (10), and $m_P = r_E \geqslant 2$, along with the requirement that $\gcd\{b, r_E\} = 1$, we obtain finitely many possibilities for the triple (j, r_E, b), as recorded in Table 3.

Table 3. The possible values of (j, r_E, b).

j	5	5	6	6	7	7	8	8	8	9	9	9
r_E	2	5	2	3	2	3	2	3	4	2	3	4
b	1	2	1	1	1	1	1	1	1	1	1	1

Analysis of Table 3: First we consider the cases where $r_E = 2$ and $b = 1$. Here P is contained in the rectangle $[-1, 1] \times [-j + 2, 2]$. Let E'' be the edge with $(0, -1) \in \mathrm{cone}(E'')$ that contains the lower right vertex $(1, 2 - j) \in E''$. If $(0, -1) \notin P$ then one immediately finds that $j = 5$ and P is a triangle. This is the triangle T_8 in Table 1. If $(0, -1) \in \partial P$ then $j \leqslant 6$, and P is either the triangle T_5,

Downloaded from https://www.cambridge.org/core. IP address: 185.31.154.38, on 21 Aug 2017 at 16:48:03, subject to the Cambridge Core terms of use, available at https://www.cambridge.org/core/terms. https://doi.org/10.1017/fms.2017.10

or one of P_6 or P_7 in Table 2. Finally, if $(0,-1) \in P^\circ$ then the Gorenstein index of E'' must be two. Therefore, $(0,-2) \in E''$, giving either the triangle T_2, or one of P_2, P_3, or P_4.

In the cases $(5,5,2)$, $(8,4,1)$, and $(9,3,1)$, we have equality in (9), hence $1 = \mathrm{Vol}(P^*) = \mathrm{Vol}(T^*)$ and so $P = T$ is uniquely determined. This gives the triangles T_1, T_4, and T_9. In the case $(6,3,1)$ the triangle $T = T_6$. In the remaining cases it is easily verified that T is not a minimal triangle with only T-singularities; this completes the proof of (iii).

Consider the cases $(6,3,1)$, $(7,3,1)$, and $(8,3,1)$. In all three cases $r_E = 3$ and $b = 1$, hence P is contained in the rectangle $[-2,1] \times [-j+3,3]$, $j \in \{6,7,8\}$. If we assume that P is not a triangle, it follows that $(0,-1) \in P^\circ$, therefore $(0,-1) \in \mathrm{cone}(E'')$ for an edge $E'' \in \mathcal{F}(P)$ containing the bottom-right vertex $(1, 3-j)$. This implies that the edge E'' has Gorenstein index two or three. Let us assume the Gorenstein index of E'' is three. Then it must have length three, and so P is not a triangle; there must exist one more vertex with first coordinate -2. However, this means that there exists a left vertical edge, contradicting minimality. Now assume that the Gorenstein index of E'' is two. Hence $(0,-2)$ is an interior point in E'', and since E'' has length two there is a unique vertex with first coordinate -1. Hence there can be at most one vertex left with first coordinate -2, excluding the vertex $(-2,3)$. Enumerating these possibilities shows that none result in a minimal Fano polygon with only T-cones.

Finally, consider the case $(9,4,1)$. We see that $(0,-2) \in P^\circ$, hence the nonvertical edge $E'' \in \mathcal{F}(P)$ containing $(1,-5)$ is of Gorenstein index either three or four. If $r_{E''} = 3$ then $(-2,1)$ is a vertex of P, and if $r_{E''} = 4$ then $(-3,-1)$ is a vertex of P. In either case P fails to have only T-cones, and so (iv) is complete. □

COROLLARY 7. *There are precisely two mutation-equivalence classes of Fano polygons with singularity content* $(4,\varnothing)$. *These classes are given by* R_{15} *and* R_{16}, *corresponding to the toric varieties* $\mathbb{F}_1$ *and* $\mathbb{P}^1 \times \mathbb{P}^1$, *respectively.*

Proof. By Theorem 5 there are only three minimal polygons with singularity content $(4,\varnothing)$: R_3, R_{15}, and R_{16}. It is easy to see that R_3 and R_{16} are mutation-equivalent. That R_{15} and R_{16} are distinct up to mutation is shown in Example 6. □

THEOREM 6. *There are ten mutation-equivalence classes of Fano polygon with residual basket* $\mathcal{B} = \varnothing$. *Representative polygons for each mutation-equivalence class are given by* R_1, R_{16}, R_{15}, R_{14}, R_{12}, R_9, R_7, R_2, T_3, *and* T_7. *These representatives are depicted in Figure* 1.

Downloaded from https://www.cambridge.org/core. IP address: 185.31.154.38, on 21 Aug 2017 at 16:48:03, subject to the Cambridge Core terms of use, available at https://www.cambridge.org/core/terms. https://doi.org/10.1017/fms.2017.10

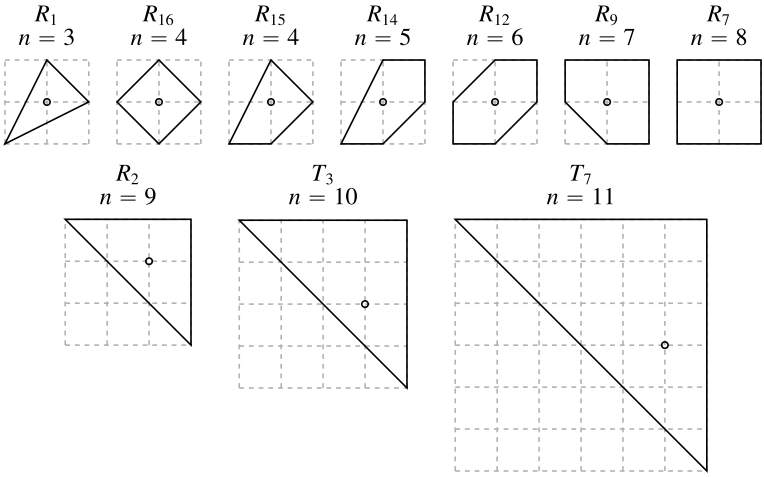

Figure 1. A representative minimal Fano polygon $P \subset N_{\mathbb{Q}}$ with singularity content $(n, \varnothing)$, for each of the 10 mutation-equivalence classes. The representatives correspond, up to the action of $\mathrm{GL}_2(\mathbb{Z})$, with the polygons marked $\star$ in Tables 2 and 4. The degree is $(-K_{X_P})^2 = 12 - n$.

Proof. Let $P, Q \subset N_{\mathbb{Q}}$ be two minimal Fano polygons as given in Theorem 5 with $\mathrm{SC}(P) = \mathrm{SC}(Q)$. With the exception of the case when $\mathrm{SC}(P) = \mathrm{SC}(Q) = (4, \varnothing)$, which is handled in Corollary 7 above, it can easily be seen that P and Q are mutation-equivalent. We do the case when $\mathrm{SC}(P) = \mathrm{SC}(Q) = (6, \varnothing)$; the remaining cases are similar. The minimal Fano polygons R_5, R_{10}, R_{11}, and R_{12} are connected via a sequence of mutations:

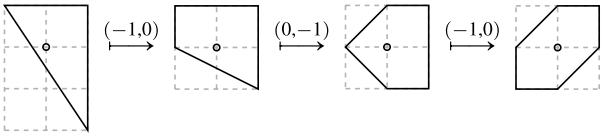

The mutations have been labelled with their corresponding primitive inner normal vector w. □

6. Finiteness of minimal Fano polygons

In this section we generalize Theorem 5 to the case when the residual basket $\mathcal{B} \neq \varnothing$.

Downloaded from https://www.cambridge.org/core. IP address: 185.31.154.38, on 21 Aug 2017 at 16:48:03, subject to the Cambridge Core terms of use, available at https://www.cambridge.org/core/terms. https://doi.org/10.1017/fms.2017.10

DEFINITION 14. Given a residual basket $\mathcal{B} \neq \varnothing$ we define

$$\begin{aligned} m_{\mathcal{B}} &:= \max\{r_\sigma \mid \sigma \in \mathcal{B}\}, \\ d_{\mathcal{B}} &:= \operatorname{lcm}\{\operatorname{denom}(A_\sigma) \mid \sigma \in \mathcal{B}\}, \\ s_{\mathcal{B}} &:= -\min(\{0\} \cup \{A_\sigma \mid \sigma \in \mathcal{B}\}), \end{aligned}$$

where r_σ is the Gorenstein index of σ, A_σ is the contribution of σ to the degree (as given in Proposition 1), and $\operatorname{denom}(x)$ denotes the denominator of $x \in \mathbb{Q}$. In the case when $\mathcal{B} = \varnothing$ we define $m_{\mathcal{B}} := 1$, $d_{\mathcal{B}} := 1$, and $s_{\mathcal{B}} := 0$.

REMARK 6. Bounding $m_{\mathcal{B}}$ automatically bounds the number of possible types of singularities that can occur in the residual basket. In particular there are only finitely many possible values of A_σ, hence $d_{\mathcal{B}}$ and $s_{\mathcal{B}}$ are bounded from above.

THEOREM 7. *There exist only a finite number of minimal Fano polygons, up to the action of* $\mathrm{GL}_2(\mathbb{Z})$*, with bounded maximum Gorenstein index* $m_{\mathcal{B}}$ *of the cones in the residual baskets* $\mathcal{B}$*.*

Proof. We assume throughout that $\mathcal{B} \neq \varnothing$, the empty case having already been considered in Theorem 5. The proof is constructive, and follows a similar structure to the proof when $\mathcal{B} = \varnothing$.

$\underline{m_P = m_{\mathcal{B}}}$: The number of possible Fano polygons with bounded maximum Gorenstein index m_P is known to be finite, up to $\mathrm{GL}_2(\mathbb{Z})$-equivalence. Algorithms for computing all such Fano polygons are described in [**28**].

$\underline{m_P > m_{\mathcal{B}}}$: Let $E \in \mathcal{F}(P)$ be an edge of maximum Gorenstein index $r_E = m_P > m_{\mathcal{B}}$. In particular $\operatorname{cone}(E)$ is a T-cone, hence $|E \cap N| = kr_E + 1$ for some $k \in \mathbb{Z}_{>0}$. After suitable change of basis we can insist that $E = \operatorname{conv}\{(-a, r_E), (b, r_E)\}$ where $a, b > 0$, $a < r_E$, and $a + b = kr_E$. Hence, as in the proof of Theorem 5, there exist k distinct points $v_i = (i - 1, 1)$, for $i = 1, \ldots, k$, where each $v_i \in \operatorname{cone}(E)^\circ$, $w_E(v_i) = -1$. Let $v \in \mathcal{V}(P)$ be a vertex of P such that $w_E(v) = \max\{w_E(v') \mid v' \in P\}$. Since P is minimal by assumption, by Corollary 5 we have that $w_E(v) \geqslant r_E$. By applying Lemma 7 with respect to v_1 and v_k we conclude that $k \leqslant 2$.

$\underline{k = 2}$: First we consider the case when $k = 2$. As in the proof of Theorem 5 we have that

$$\begin{aligned} P = \operatorname{conv}\{(-a, r_E), (-a + 2r_E, r_E), (-a, -r_E)\}, \\ \text{where } 0 < a < r_E,\ \gcd\{a, r_E\} = 1. \end{aligned}$$

Let E_1 and E_2 be the two edges of P distinct from the horizontal edge E, where $r_{E_1} = a$ and $r_{E_2} = r_E - a$. Since at least one of these two edges has Gorenstein

Downloaded from https://www.cambridge.org/core. IP address: 185.31.154.38, on 21 Aug 2017 at 16:48:03, subject to the Cambridge Core terms of use, available at https://www.cambridge.org/core/terms. https://doi.org/10.1017/fms.2017.10

index $m_{\mathcal{B}}$, by symmetry we can assume that $a = m_{\mathcal{B}}$. The edge E_2 is of length $2r_E$, giving $2r_E = j(r_E - m_{\mathcal{B}}) + l$ for some $j \in \mathbb{Z}_{\geqslant 0}$, $0 \leqslant l < r_E - m_{\mathcal{B}}$.

If $l = 0$ then $jm_{\mathcal{B}} = (j-2)r_E$, and $\gcd\{m_{\mathcal{B}}, r_E\} = 1$ implies that $r_E \mid j$. Writing $j = j'r_E$ for some $j' \in \mathbb{Z}_{\geqslant 0}$ we see that $2 = j'(r_E - m_{\mathcal{B}})$ and hence $r_E = m_{\mathcal{B}} + 1$ or $r_E = m_{\mathcal{B}} + 2$. If $l > 0$ then $r_E - m_{\mathcal{B}} \leqslant m_{\mathcal{B}}$, and so $r_E < 2m_{\mathcal{B}}$ (the case of equality being excluded by primitivity). Hence in either case the number of possible minimal polygons is finite.

$k = 1$: We now consider the case when $k = 1$. Once again we subdivide this into two cases depending on whether there exists an edge $E' \in \mathcal{F}(P)$ parallel to E.

Edge E' parallel to E: First we assume that there exists an edge $E' \in \mathcal{F}(P)$ such that v is a vertex of E', and E' is parallel to E. If $\operatorname{cone}(E')$ contains a residual component then $r_{E'} \leqslant m_{\mathcal{B}}$. By minimality $r_E \leqslant m_{\mathcal{B}}$, which is a contradiction. Therefore, $\operatorname{cone}(E')$ must be of class T, and by minimality we see that $r_{E'} = r_E$. As in the proof of Theorem 5 we conclude that P is a rectangle:

$$P = \operatorname{conv}\{(-a, r_E), (-a + r_E, r_E), (-a, -r_E), (-a + r_E, -r_E)\}.$$

Since one of the two vertical edges must contain a residual component at height $m_{\mathcal{B}}$, without loss of generality we may assume that $a = m_{\mathcal{B}}$, hence $2r_E = jm_{\mathcal{B}} + l$ for some $j \in \mathbb{Z}_{\geqslant 0}$, $0 < l < m_{\mathcal{B}}$. Notice that if $j = 0$ then $2r_E = l < m_{\mathcal{B}}$, a contradiction. Hence $j > 0$. The second vertical edge lies at height $r_E - m_{\mathcal{B}}$, and by Corollary 5 we have that $2m_{\mathcal{B}} \leqslant r_E$. Hence $2r_E = j'(r_E - m_{\mathcal{B}}) + l'$ for some $j' \in \mathbb{Z}_{\geqslant 0}$, $0 \leqslant l' < r_E - m_{\mathcal{B}}$. If $j' = 0$ then $2r_E = l' < r_E - m_{\mathcal{B}}$, a contradiction. If $j > 0$ then, by minimality, $r_E \leqslant 2m_{\mathcal{B}}$, implying that $r_E = 2m_{\mathcal{B}}$. But this contradicts primitivity, hence this case does not occur.

No edge parallel to E: We now assume that v is the unique point in P such that $w_E(v) = \max\{w_E(v') \mid v' \in P\}$. Once again we subdivide this into two cases, depending on whether there exists a vertical edge $E' \in \mathcal{F}(P)$ with vertex v.

E' not vertical: This proof in this case is identical to that of Theorem 5: it results in no minimal polygons.

E' vertical: Without loss of generality we may assume that there is a vertical edge $E' \in \mathcal{F}(P)$ with vertices v and (b, r_E). Hence $v = (b, r_E - jb - l)$ for some $j \in \mathbb{Z}_{\geqslant 0}$, $0 \leqslant l < b$. By minimality of E,

$$2r_E \leqslant jb + l. \tag{11}$$

Notice that if $j = 0$ then $2r_E \leqslant l < m_{\mathcal{B}}$, a contradiction. Hence $j > 0$ and, by minimality of E',

$$2b \leqslant r_E. \tag{12}$$

$l = 0$: When $l = 0$, inequalities (11) and (12) imply that $j \geqslant 4$.

Downloaded from https://www.cambridge.org/core. IP address: 185.31.154.38, on 21 Aug 2017 at 16:48:03, subject to the Cambridge Core terms of use, available at https://www.cambridge.org/core/terms. https://doi.org/10.1017/fms.2017.10

$\underline{j = 4}$: Assume that $j = 4$. Then $2b = r_E$, so $\gcd\{b, r_E\} = 1$ implies that $r_E = 2$ and $b = 1$. Hence P is contained in the rectangle $[-1, 1] \times [-2, 2]$. This contains only four possible polygons, all of which have $m_P \leqslant 3$, contradicting $m_P > m_{\mathcal{B}} \geqslant 3$. Hence this case does not occur.

$\underline{j \geqslant 5}$: As in the proof of Theorem 5, $\mathbf{0}$ is contained in the strict interior of the triangle

$$T := \operatorname{conv}\{(b - r_E, r_E), (b, r_E), (b, r_E - jb)\} \subset P.$$

As before, the area of the dual triangle is given by

$$\operatorname{Vol}(T^*) = \frac{j}{jbr_E - jb^2 - r_E^2}.$$

By Proposition 1, $\operatorname{Vol}(P^*) \in 1/d_{\mathcal{B}} \cdot \mathbb{Z}_{>0}$, hence $1/d_{\mathcal{B}} \leqslant \operatorname{Vol}(P^*) \leqslant \operatorname{Vol}(T^*)$. Let $b = r_E q$, where $2/j \leqslant q \leqslant 1/2$, by (11) and (12). Then $r_E^2(-jq^2 + jq - 1) \leqslant jd_{\mathcal{B}}$, and by considering the minimum value achieved by the quadratic in q on the left-hand side of this inequality we obtain

$$r_E^2 \leqslant \frac{j^2 d_{\mathcal{B}}}{j - 4} = \left(j + 4 + \frac{16}{j - 4}\right) d_{\mathcal{B}} \leqslant (j + 20) d_{\mathcal{B}}. \tag{13}$$

Notice that the number of edges of P distinct from E and E' can be at most $r_E + 1$. By Proposition 1 we obtain that $12 - 1 - j + (r_E + 1)s_{\mathcal{B}} \geqslant \operatorname{Vol}(P^*) > 0$. Hence

$$j < 11 + (r_E + 1)s_{\mathcal{B}}. \tag{14}$$

Combining inequalities (13) and (14) gives $r_E^2 < (31 + (r_E + 1)s_{\mathcal{B}})d_{\mathcal{B}}$, which implies that

$$r_E < \frac{s_{\mathcal{B}} d_{\mathcal{B}} + \sqrt{(s_{\mathcal{B}} d_{\mathcal{B}})^2 + 4d_{\mathcal{B}}(s_{\mathcal{B}} + 31)}}{2}. \tag{15}$$

Since j is bounded by (14), the result follows.

$\underline{l > 0}$: Finally, let us consider the case when the edge E' contributes a residual singularity to the basket $\mathcal{B}$. Notice that if we had equality in (12), primitivity forces $r_E = 2$ and $b = 1$, and so $l = 0$, which is a contradiction. Hence we conclude that the inequality is strict:

$$2b < r_E. \tag{16}$$

Once again we find that $j \geqslant 4$.

Consider the triangle

$$T := \operatorname{conv}\{(b - r_E, r_E), (b, r_E), (b, r_E - jb - l)\} \subset P.$$

Downloaded from https://www.cambridge.org/core. IP address: 185.31.154.38, on 21 Aug 2017 at 16:48:03, subject to the Cambridge Core terms of use, available at https://www.cambridge.org/core/terms. https://doi.org/10.1017/fms.2017.10

One can check that $\mathbf{0} \in T^\circ$, so T is a Fano triangle with $\mathrm{Vol}(T) = r_E(jb+l)$. Moreover, the weights

$$(b(jb+l), (jb+l)(r_E-b) - r_E^2, r_E^2) \in \mathbb{Z}^3_{>0}$$

satisfy the conditions of Lemma 6 (that the second weight is strictly positive follows from (11) and (16): $(jb+l)(r_E-b)-r_E^2 \geqslant 2r_E^2-2r_Eb-r_E^2 = r_E(r_E-2b) > 0$). Hence

$$\mathrm{Vol}(T^*) = \frac{jb+l}{b(jb+l)(r_E-b) - br_E^2} < \frac{j+1}{(jb+l)(r_E-b)-r_E^2}.$$

Recalling, as above, that $1/d_{\mathcal{B}} \leqslant \mathrm{Vol}(P^*) \leqslant \mathrm{Vol}(T^*)$ we obtain:

$$(jb+l)(r_E-b) - r_E^2 < (j+1)d_{\mathcal{B}}. \tag{17}$$

The quadratic in b on the left-hand side of (17) is strictly positive in the range $(2r_E-l)/j \leqslant b < r_E/2$, and obtains its minimum value when $b = (2r_E-l)/j$. Hence (17) gives:

$$(j-4)r_E^2 + 2lr_E < j(j+1)d_{\mathcal{B}}. \tag{18}$$

We consider the cases $j = 4$ and $j > 4$ separately.

$\underline{j=4}$: When $j = 4$ inequalities (11) and (16) give $r_E - l/2 \leqslant 2b < r_E$. Hence if $l = 1$ this case does not occur. If $l > 1$ then (18) gives us that $r_E < 10d_{\mathcal{B}}$, resulting in only finitely many possibilities.

$\underline{j \geqslant 5}$: When $j \geqslant 5$ inequality (18) implies that

$$r_E^2 < \frac{j(j+1)d_{\mathcal{B}}}{j-4} = \left(j+5+\frac{20}{j-4}\right)d_{\mathcal{B}} \leqslant (j+25)d_{\mathcal{B}}. \tag{19}$$

Notice that the number of edges of P distinct from E and E' is at most r_E+1, so by Proposition 1 we have that $12-1-j+(r_E+2)s_{\mathcal{B}} \geqslant \mathrm{Vol}(P^*) > 0$. Hence

$$j < 11 + (r_E+2)s_{\mathcal{B}}. \tag{20}$$

Combining inequalities (19) and (20) gives $r_E^2 < (36+(r_E+2)s_{\mathcal{B}})d_{\mathcal{B}}$. This implies that

$$r_E < \frac{s_{\mathcal{B}}d_{\mathcal{B}} + \sqrt{(s_{\mathcal{B}}d_{\mathcal{B}})^2 + 4d_{\mathcal{B}}(2s_{\mathcal{B}}+36)}}{2}. \tag{21}$$

Since j is bounded by (20) we have only finitely many possible minimal polygons. □

Downloaded from https://www.cambridge.org/core. IP address: 185.31.154.38, on 21 Aug 2017 at 16:48:03, subject to the Cambridge Core terms of use, available at https://www.cambridge.org/core/terms. https://doi.org/10.1017/fms.2017.10

7. Minimal Fano polygons with $\mathcal{B} = \{m \times 1/3(1,1)\}$

In this section we apply Theorem 7 in order to classify all minimal Fano polygons with residual basket $\mathcal{B}$ containing only singularities of type $1/3(1,1)$. We find 65 minimal Fano polygons (Theorem 8 and Table 4), which result in 26 mutation-equivalence classes (Theorem 9 and Figure 2). These mutation-equivalence classes correspond exactly with the classification of Corti–Heuberger of qG-deformation-equivalence classes of del Pezzo surfaces of class TG with $m \times 1/3(1,1)$ singular points [**14**].

In some sense $1/3(1,1)$ is the 'simplest' residual singularity. Up to change of basis, the corresponding cone is given by $C := \mathrm{cone}\{(1,0),(2,3)\}$. The length of the line segment joining the primitive generators of the rays of C is one. The Gorenstein index is three. By Example 5 any Fano polygon P with singularity content $(n, \{m \times 1/3(1,1)\})$ gives rise to a toric surface X_P with degree

$$(-K_{X_P})^2 = 12 - n - \frac{5m}{3}.$$

In the notation of Definition 14, $m_{\mathcal{B}} = d_{\mathcal{B}} = 3$ and $s_{\mathcal{B}} = 0$.

THEOREM 8. *Let $P \subset N_{\mathbb{Q}}$ be a minimal Fano polygon with residual basket $\mathcal{B} = \{m \times 1/3(1,1)\}$, for some $m \geqslant 1$. Then, up to $\mathrm{GL}_2(\mathbb{Z})$-equivalence, P is one of the 65 polygons listed in Table 4 (page 41).*

Proof. To derive the classification, we follow the proof of Theorem 7.

$\underline{m_P = 3}$: Techniques for classifying all Fano polygons with given maximum Gorenstein index m_P (or with given Gorenstein index r) are described in [**28**]. The resulting classifications for low index are available online [**10**], and it is a simple process to sift these results for the minimal polygons we require. There are precisely 60 such polygons. These are the polygons in Table 4, excluding numbers (1.1), (1.2), (1.3), (1.4), and (2.6).

$\underline{m_P > 3, k = 2}$: In this case P is a triangle with vertices $(-3, r_E)$, $(-3+2r_E, r_E)$, and $(-3, -r_E)$, where $r_E = m_P$ equals 4 or 5. We require that $2r_E \equiv 1 \pmod 3$, which excludes $r_E = 4$. This gives polygon number (1.1) in Table 4.

$\underline{m_P = r_E > 3, k = 1}$, no edge parallel to E, E' vertical, $l = 0$, $j \geqslant 5$: Now P has vertices $(b - r_E, r_E)$, (b, r_E), $(b, r_E - jb)$, and is contained in the rectangle $[b - r_E, b] \times [r_E - jb, r_E]$ where $5 \leqslant j < 11$, by (14), $3 < r_E \leqslant 9$, by (15), and $2r_E/j \leqslant b \leqslant r_E/2$ by (11) and (12). This gives three minimal polygons: numbers (1.2), (1.3), and (2.6) in Table 4.

$\underline{m_P = r_E > 3, k = 1}$, no edge parallel to E, E' vertical, $l > 0$, $j \geqslant 5$: Now P has vertices $(b - r_E, r_E)$, (b, r_E), $(b, r_E - jb - 1)$, and is contained in the rectangle

Downloaded from https://www.cambridge.org/core. IP address: 185.31.154.38, on 21 Aug 2017 at 16:48:03, subject to the Cambridge Core terms of use, available at https://www.cambridge.org/core/terms. https://doi.org/10.1017/fms.2017.10

$[b - r_E, b] \times [r_E - jb - 1, r_E]$ where $5 \leqslant j < 11$, by (20), $3 < r_E \leqslant 10$, by (21), and $2r_E/j \leqslant b < r_E/2$, by (11) and (16). This gives polygon number (1.4) in Table 4. □

We now use the minimal polygons from Theorem 8 to generate a complete list of mutation classes of Fano polygons P with $\mathrm{SC}(P) = (n, \{m \times 1/3(1, 1)\})$, $m \geqslant 1$. For future reference we recall some of the polygons from Table 4:

LEMMA 8. *There are exactly two mutation-equivalence classes of Fano polygons with singularity content* $(6, \{2\times 1/3(1, 1)\})$. *The mutation-equivalence classes are generated by*

$$P_{12} = \mathrm{conv}\{(6, 1), (0, 1), (-3, -1)\}$$
$$\textit{and} \quad P_{13} = \mathrm{conv}\{(1, 0), (-1, 3), (-2, 3), (1, -3)\}.$$

Proof. Notice that the six primitive T-cones in P_{12} are all contributed by the (cone over the) edge E with inner normal vector $(0, -1) \in M$. Hence $\Gamma_{P_{12}}$ is a one-dimensional sublattice of M. The polygon P_{13} has primitive T-cones contributed by those edges with inner normal vectors $(-1, 0)$ and $(2, 1) \in M$, hence $\Gamma_{P_{13}}$ equals M. By Lemma 3 we conclude that P_{12} cannot be mutation-equivalent to P_{13}. Denote the polygons with numbers (12.2), (12.3), and (12.4) in Table 4 by $P_{12.2}$, $P_{12.3}$, and $P_{12.4}$ respectively. These three polygons are mutation-equivalent to P_{12}, corresponding to number (12.1) in Table 4, via:

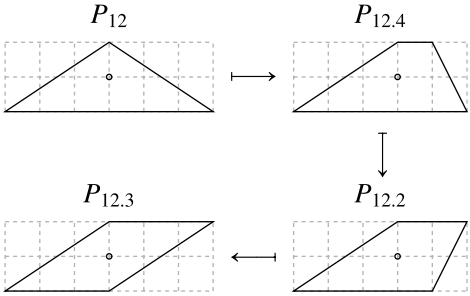

For each mutation the primitive inner normal vector used is $w = (0, 1)$. Note that the polygon depicted for P_{12} is $\mathrm{GL}_2(\mathbb{Z})$-equivalent to P_{12} as defined above. □

LEMMA 9. *There are exactly two mutation-equivalence classes of Fano polygons with singularity content* $(5, \{1\times 1/3(1, 1)\})$. *The mutation-equivalence classes are generated by*

$$P_{21} = \mathrm{conv}\{(4, 1), (0, 1), (-3, -1)\}$$
$$\textit{and} \quad P_{22} = \mathrm{conv}\{(3, 1), (0, 1), (-1, 0), (0, -1)\}.$$

Downloaded from https://www.cambridge.org/core. IP address: 185.31.154.38, on 21 Aug 2017 at 16:48:03, subject to the Cambridge Core terms of use, available at https://www.cambridge.org/core/terms. https://doi.org/10.1017/fms.2017.10

Proof. The primitive inner normal vectors to the edges of P_{21} which contribute primitive T-cones are $(0,-1)$ and $(-2,7) \in M$. These generate an index-two sublattice $\Gamma_{P_{21}}$ of M. In the case of P_{22} the relevant inner normal vectors are $(1,1)$, $(1,-1)$, and $(0,-1) \in M$, and we have that $[M : \Gamma_{P_{22}}] = 1$. By Lemma 3 we conclude that P_{21} and P_{22} lie in distinct mutation-equivalence classes. We leave it to the reader to verify that the polygons with numbers (21.2), (21.3) (respectively, (22.2)) in Table 4 are mutation-equivalent to (21.1) (respectively, (22.1)), which is P_{21} (respectively, P_{22}). □

THEOREM 9. *There are* 26 *mutation-equivalence classes of Fano polygons with singularity content* $(n, \{m \times 1/3(1,1)\})$, $m \geqslant 1$. *Representative polygons for each mutation-equivalence class are depicted in Figure* 2 *(page* 40*).*

Proof. The values n and m distinguishes every mutation class of Fano polygons with $1/3(1,1)$ singularities except in the cases $n = 6$, $m = 2$ and $n = 5$, $m = 1$. These two exceptional cases are handled in Lemmas 8 and 9 above. We shall show that the minimal polygons in Table 4 with $n = 9$, $m = 1$ are connected by mutation; the remaining cases are similar. There are four minimal polygons to consider, with numbers (4.1), (4.2), (4.3), and (4.4) in Table 4. Denote these polygons by $P_{4.1}$, $P_{4.2}$, $P_{4.3}$, and $P_{4.4}$, respectively. Then, up to $\mathrm{GL}_2(\mathbb{Z})$-equivalence, we have the sequence of mutations:

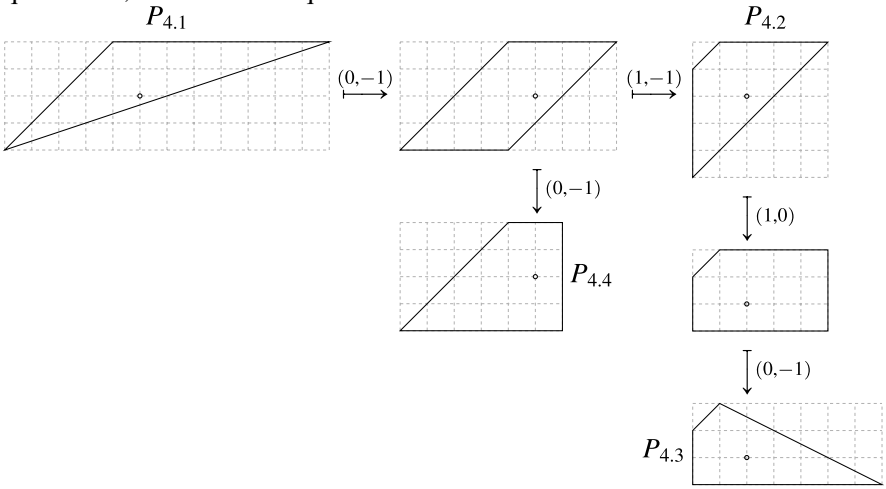

The mutations have been labelled with their corresponding primitive inner normal vector w. □

Downloaded from https://www.cambridge.org/core. IP address: 185.31.154.38, on 21 Aug 2017 at 16:48:03, subject to the Cambridge Core terms of use, available at https://www.cambridge.org/core/terms. https://doi.org/10.1017/fms.2017.10

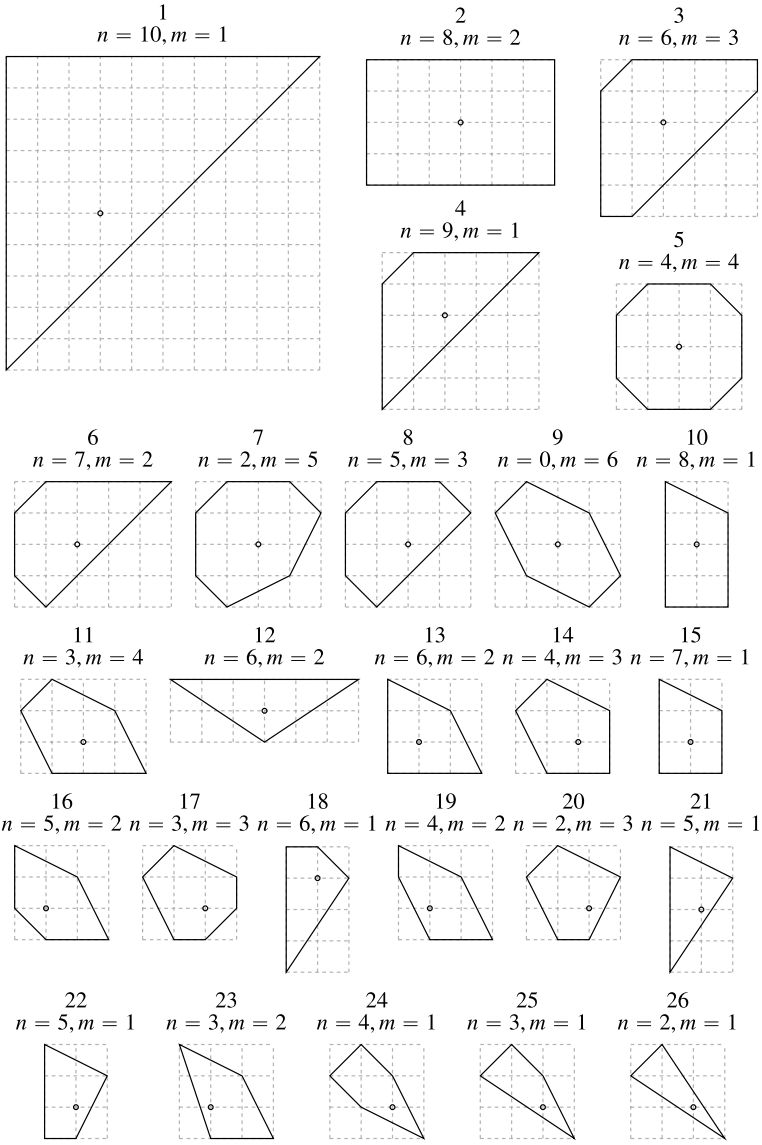

Figure 2. Representative minimal Fano polygons P with singularity content $(n, \{m \times 1/3(1, 1)\})$, $m \geqslant 1$, for each of the 26 mutation-equivalence classes. The representatives correspond, up to the action of $\mathrm{GL}_2(\mathbb{Z})$, with the polygons marked $\star$ in Table 4. The degree is $(-K_{X_P})^2 = 12 - n - 5m/3$.

Downloaded from https://www.cambridge.org/core. IP address: 185.31.154.38, on 21 Aug 2017 at 16:48:03, subject to the Cambridge Core terms of use, available at https://www.cambridge.org/core/terms. https://doi.org/10.1017/fms.2017.10

Downloaded from https://www.cambridge.org/core. IP address: 185.31.154.38, on 21 Aug 2017 at 16:48:03, subject to the Cambridge Core terms of use, available at https://www.cambridge.org/core/terms. https://doi.org/10.1017/fms.2017.10

Table 4. The 65 minimal Fano polygons $P \subset N_{\mathbb{Q}}$ with singularity content $(n, \{m \times 1/3(1,1)\})$, $m \geqslant 1$, vertices $\mathcal{V}(P)$, and maximum Gorenstein index m_P, up to the action of $\mathrm{GL}_2(\mathbb{Z})$. The degrees $(-K_{X_P})^2 = 12-n-5m/3$ of the corresponding toric varieties are also given. The polygons are partitioned into 26 mutation-equivalence classes; the invariants n and m completely determine the mutation-equivalence class except when $n = 6$, $m = 2$, $(-K_{X_P})^2 = 8/3$, and when $n = 5$, $m = 1$, $(-K_{X_P})^2 = 16/3$. See Theorems 8 and 9. Those P marked with $\star$ are chosen as the representative polygon in the mutation-equivalence class, and are depicted in Figure 2 (page 40).

#	$\mathcal{V}(P)$	m_P	n	m	$(-K_{X_P})^2$
$\star$1.1	$(7,5),(-3,5),(-3,-5)$	5	10	1	$\frac{1}{3}$
1.2	$(2,5),(-3,5),(-3,4),(2,-11)$	5	10	1	$\frac{1}{3}$
1.3	$(2,7),(-5,7),(2,-7)$	7	10	1	$\frac{1}{3}$
1.4	$(3,8),(-5,8),(3,-8)$	8	10	1	$\frac{1}{3}$
2.1	$(11,2),(-1,2),(-5,-2)$	3	8	2	$\frac{2}{3}$
2.2	$(5,2),(-1,2),(-2,1),(-2,-5)$	3	8	2	$\frac{2}{3}$
2.3	$(5,2),(-1,2),(-5,-2),(1,-2)$	3	8	2	$\frac{2}{3}$
$\star$2.4	$(3,2),(-1,2),(-5,-2),(3,-2)$	3	8	2	$\frac{2}{3}$
2.5	$(1,2),(-1,2),(-5,-2),(5,-2)$	3	8	2	$\frac{2}{3}$
2.6	$(2,5),(-3,5),(-3,4),(1,-4),(2,-5)$	5	8	2	$\frac{2}{3}$
3.1	$(7,2),(-1,2),(-2,1),(-2,-1),(-1,-2)$	3	6	3	1
$\star$3.2	$(3,1),(3,2),(-1,2),(-2,1),(-2,-3),(-1,-3)$	3	6	3	1
3.3	$(2,1),(1,2),(-1,2),(-2,1),(-2,-1),(2,-5)$	3	6	3	1

Continued on next page.

Downloaded from https://www.cambridge.org/core. IP address: 185.31.154.38, on 21 Aug 2017 at 16:48:03, subject to the Cambridge Core terms of use, available at https://www.cambridge.org/core/terms. https://doi.org/10.1017/fms.2017.10

Table 4. Continued.

#	$\mathcal{V}(P)$	m_P	n	m	$(-K_{X_P})^2$
4.1	$(7,2),(-1,2),(-5,-2)$	3	9	1	$\frac{4}{3}$
⋆4.2	$(3,2),(-1,2),(-2,1),(-2,-3)$	3	9	1	$\frac{4}{3}$
4.3	$(1,2),(-1,2),(-2,1),(1,-5)$	3	9	1	$\frac{4}{3}$
4.4	$(1,2),(-1,2),(-5,-2),(1,-2)$	3	9	1	$\frac{4}{3}$
5.1	$(5,2),(-1,2),(-2,1),(-1,-1),(1,-2)$	3	4	4	$\frac{4}{3}$
5.2	$(3,1),(3,2),(-1,2),(-2,1),(-2,-1),(-1,-2),(1,-1)$	3	4	4	$\frac{4}{3}$
⋆5.3	$(2,1),(1,2),(-1,2),(-2,1),(-2,-1),(-1,-2),(1,-2),(2,-1)$	3	4	4	$\frac{4}{3}$
6.1	$(1,0),(2,3),(-1,3),(-1,-3)$	3	7	2	$\frac{5}{3}$
6.2	$(5,2),(-1,2),(-2,1),(1,-2)$	3	7	2	$\frac{5}{3}$
6.3	$(5,2),(-1,2),(-5,-2),(-1,-1)$	3	7	2	$\frac{5}{3}$
⋆6.4	$(2,1),(1,2),(-1,2),(-2,1),(-2,-3)$	3	7	2	$\frac{5}{3}$
6.5	$(1,2),(-1,2),(-2,1),(-1,-1),(1,-3)$	3	7	2	$\frac{5}{3}$
⋆7.1	$(2,1),(1,2),(-1,2),(-2,1),(-2,-1),(-1,-2),(1,-1)$	3	2	5	$\frac{5}{3}$
8.1	$(1,2),(-1,2),(-2,1),(-1,-1),(1,-2)$	3	5	3	2
⋆8.2	$(2,1),(1,2),(-1,2),(-2,1),(-2,-1),(-1,-2)$	3	5	3	2
⋆9.1	$(1,0),(-1,3),(-2,3),(-1,0),(1,-3),(2,-3)$	3	0	6	2

Continued on next page.

Table 4. Continued.

#	$\mathcal{V}(P)$	m_P	n	m	$(-K_{X_P})^2$
10.1	$(7,1),(0,1),(-4,-1)$	3	8	1	$\frac{7}{3}$
10.2	$(5,2),(-1,2),(-1,0),(1,-2)$	3	8	1	$\frac{7}{3}$
10.3	$(1,1),(0,1),(-4,-1),(2,-1)$	3	8	1	$\frac{7}{3}$
10.4	$(2,1),(0,1),(-4,-1),(1,-1)$	3	8	1	$\frac{7}{3}$
⋆10.5	$(3,1),(0,1),(-4,-1),(0,-1)$	3	8	1	$\frac{7}{3}$
10.6	$(1,2),(-1,2),(-2,1),(1,-2)$	3	8	1	$\frac{7}{3}$
⋆11.1	$(1,0),(-1,3),(-2,3),(-1,0),(1,-3)$	3	3	4	$\frac{7}{3}$
⋆12.1	$(6,1),(0,1),(-3,-1)$	3	6	2	$\frac{8}{3}$
12.2	$(2,1),(0,1),(-3,-1),(1,-1)$	3	6	2	$\frac{8}{3}$
12.3	$(3,1),(0,1),(-3,-1),(0,-1)$	3	6	2	$\frac{8}{3}$
12.4	$(1,1),(0,1),(-3,-1),(2,-1)$	3	6	2	$\frac{8}{3}$
⋆13.1	$(1,0),(-1,3),(-2,3),(1,-3)$	3	6	2	$\frac{8}{3}$
⋆14.1	$(-1,3),(-2,3),(-1,0),(1,-3),(1,-1)$	3	4	3	3
15.1	$(5,1),(0,1),(-3,-1)$	3	7	1	$\frac{10}{3}$
15.2	$(1,1),(0,1),(-3,-1),(1,-1)$	3	7	1	$\frac{10}{3}$
⋆15.3	$(2,1),(0,1),(-3,-1),(0,-1)$	3	7	1	$\frac{10}{3}$
15.4	$(5,2),(-1,2),(-1,1),(0,-1),(1,-2)$	3	7	1	$\frac{10}{3}$

Continued on next page.

Downloaded from https://www.cambridge.org/core. IP address: 185.31.154.38, on 21 Aug 2017 at 16:48:03, subject to the Cambridge Core terms of use, available at https://www.cambridge.org/core/terms. https://doi.org/10.1017/fms.2017.10

Table 4. Continued.

#	$\mathcal{V}(P)$	m_P	n	m	$(-K_{X_P})^2$
⋆16.1	$(-1,3),(-2,3),(-1,0),(1,-2),(1,-1)$	3	5	2	$\frac{11}{3}$
⋆17.1	$(0,1),(-1,3),(-2,3),(-1,0),(1,-3),(1,-2)$	3	3	3	4
⋆18.1	$(4,1),(0,1),(-1,0),(-1,-1)$	3	6	1	$\frac{13}{3}$
18.2	$(1,0),(1,1),(0,1),(-3,-1),(0,-1)$	3	6	1	$\frac{13}{3}$
18.3	$(2,1),(0,1),(-1,0),(-1,-1),(1,-1)$	3	6	1	$\frac{13}{3}$
18.4	$(5,2),(-1,2),(-5,-2),(-2,-1)$	3	6	1	$\frac{13}{3}$
18.5	$(5,2),(-1,2),(-1,1),(1,-2)$	3	6	1	$\frac{13}{3}$
⋆19.1	$(0,1),(-1,3),(-2,3),(-1,0),(1,-2)$	3	4	2	$\frac{14}{3}$
⋆20.1	$(0,1),(-1,3),(-2,3),(-1,0),(1,-3)$	3	2	3	5
⋆21.1	$(4,1),(0,1),(-3,-1)$	3	5	1	$\frac{16}{3}$
21.2	$(2,1),(0,1),(-3,-1),(-1,-1)$	3	5	1	$\frac{16}{3}$
21.3	$(1,1),(0,1),(-3,-1),(0,-1)$	3	5	1	$\frac{16}{3}$
⋆22.1	$(3,1),(0,1),(-1,0),(0,-1)$	3	5	1	$\frac{16}{3}$
22.2	$(1,0),(1,1),(0,1),(-3,-1),(-1,-1)$	3	5	1	$\frac{16}{3}$
⋆23.1	$(-1,3),(-2,3),(-1,0),(1,-2)$	3	3	2	$\frac{17}{3}$
24.1	$(2,1),(0,1),(-1,0),(1,-1)$	3	4	1	$\frac{19}{3}$

Continued on next page.

Downloaded from https://www.cambridge.org/core. IP address: 185.31.154.38, on 21 Aug 2017 at 16:48:03, subject to the Cambridge Core terms of use, available at https://www.cambridge.org/core/terms. https://doi.org/10.1017/fms.2017.10

Table 4. Continued.

#	$\mathcal{V}(P)$	m_P	n	m	$(-K_{X_P})^2$
⋆24.2	$(1,0),(1,1),(0,1),(-3,-1),(-2,-1)$	3	4	1	$\frac{19}{3}$
⋆25.1	$(1,0),(1,1),(0,1),(-3,-1)$	3	3	1	$\frac{22}{3}$
⋆26.1	$(-1,3),(-2,3),(1,-2)$	3	2	1	$\frac{25}{3}$

Downloaded from https://www.cambridge.org/core. IP address: 185.31.154.38, on 21 Aug 2017 at 16:48:03, subject to the Cambridge Core terms of use, available at https://www.cambridge.org/core/terms. https://doi.org/10.1017/fms.2017.10

REMARK 7. The choice of representative for each of the 26 mutation-equivalence classes depicted in Figure 2 is not arbitrary. Where possible we chose minimal polygons that are compatible with 'Laurent inversion' [13], a technique for building a toric complete intersection model directly from the polygon. These models are then used by Corti–Heuberger in their classification [14] of del Pezzo surfaces with $1/3(1, 1)$ singularities.

Acknowledgements

This work was started at the PRAGMATIC 2013 Research School in Algebraic Geometry and Commutative Algebra, 'Topics in Higher Dimensional Algebraic Geometry', held in Catania, Italy, during September 2013. We are very grateful to Alfio Ragusa, Francesco Russo, and Giuseppe Zappalà, the organizers of the PRAGMATIC school, for creating such a wonderful atmosphere in which to work. We thank Tom Coates and Alessio Corti for many useful conversations, and Daniel Cavey for pointing out that we had overlooked polygon (1.4) in Table 4 in an early draft of this paper. The majority of this paper was written during a visit by AK to Stockholm University, supported by BN's Start-up Grant. AK is supported by EPSRC Fellowship EP/N022513/1. BN is an affiliated researcher with Stockholm University and partially supported by the Vetenskapsrådet grant NT:2014-3991. TP is supported by an EPSRC Prize Studentship.

References

[1] M. Akhtar, T. Coates, A. Corti, L. Heuberger, A. M. Kasprzyk, A. Oneto, A. Petracci, T. Prince and K. Tveiten, 'Mirror symmetry and the classification of orbifold del Pezzo surfaces', *Proc. Amer. Math. Soc.* **144**(2) (2016), 513–527.

[2] M. Akhtar, T. Coates, S. Galkin and A. M. Kasprzyk, 'Minkowski polynomials and mutations', *SIGMA Symmetry Integrability Geom. Methods Appl.* **8** (2012), Paper 094, 17.

[3] M. Akhtar and A. M. Kasprzyk, 'Singularity content', Preprint (2014), arXiv:1401.5458 [math.AG].

[4] M. Akhtar and A. M. Kasprzyk, 'Mutations of fake weighted projective planes', *Proc. Edinb. Math. Soc.* (2) **59**(2) (2016), 271–285.

[5] D. Auroux, 'Mirror symmetry and T-duality in the complement of an anticanonical divisor', *J. Gökova Geom. Topol. GGT* **1** (2007), 51–91.

[6] G. Averkov, J. Krümpelmann and B. Nill, 'Largest integral simplices with one interior integral point: solution of Hensley's conjecture and related results', *Adv. Math.* **274** (2015), 118–166.

[7] V. V. Batyrev, 'Higher dimensional toric varieties with ample anticanonical class', PhD Thesis, Moscow State University, 1985, Text in Russian.

[8] V. V. Batyrev, 'Toric degenerations of Fano varieties and constructing mirror manifolds', in *The Fano Conference* (Univ. Torino, Turin, 2004), 109–122.

Downloaded from https://www.cambridge.org/core. IP address: 185.31.154.38, on 21 Aug 2017 at 16:48:03, subject to the Cambridge Core terms of use, available at https://www.cambridge.org/core/terms. https://doi.org/10.1017/fms.2017.10

[9] I. N. Bernšteĭn, I. M. Gel′fand and V. A. Ponomarev,‘Coxeter functors, and Gabriel’s theorem’, *Uspekhi Mat. Nauk* **28**(2(170)) (1973), 19–33.
[10] G. Brown and A. M. Kasprzyk, The graded ring database, online database, http://www.grdb.co.uk/.
[11] T. Coates, A. Corti, S. Galkin, V. Golyshev and A. M. Kasprzyk, ‘Mirror symmetry and Fano manifolds’, in *European Congress of Mathematics Kraków, 2–7 July, 2012* (Eur. Math. Soc., Zürich, 2014), 285–300.
[12] T. Coates, A. Corti, S. Galkin and A. Kasprzyk, ‘Quantum periods for 3-dimensional Fano manifolds’, *Geom. Topol.* **20**(1) (2016), 103–256.
[13] T. Coates, A. M. Kasprzyk and T. Prince, ‘Laurent inversion’, Preprint (2017), arXiv:1707.05842 [math.AG].
[14] A. Corti and L. Heuberger, ‘Del Pezzo surfaces with $\frac{1}{3}(1,1)$ points’, *Manuscripta Math.* **153**(1–2) (2017), 71–118.
[15] D. I. Dais, ‘Classification of toric log del Pezzo surfaces having Picard number 1 and index $\leqslant 3$’, *Results Math.* **54**(3–4) (2009), 219–252.
[16] V. V. Fock and A. B. Goncharov, ‘Cluster ensembles, quantization and the dilogarithm. II. The intertwiner’, in *Algebra, Arithmetic, and Geometry: in Honor of Yu. I. Manin.,* Vol. I, Progress in Mathematics, 269 (Birkhäuser Boston Inc., Boston, MA, 2009), 655–673.
[17] S. Fomin and A. Zelevinsky, ‘Cluster algebras. I. Foundations’, *J. Amer. Math. Soc.* **15**(2) (2002), 497–529. (electronic).
[18] W. Fulton, *Introduction to Toric Varieties*, Annals of Mathematics Studies, 131 (Princeton University Press, Princeton, NJ, 1993), The William H. Roever Lectures in Geometry.
[19] S. Galkin and A. Usnich, ‘Laurent phenomenon for Ginzburg-Landau potential’, *IPMU Preprint* 10-0100, 2010.
[20] M. Gross, P. Hacking and S. Keel, ‘Birational geometry of cluster algebras’, Preprint (2013), arXiv:1309.2573 [math.AG].
[21] M. Gross, P. Hacking and S. Keel, ‘Mirror symmetry for log Calabi–Yau surfaces I’, *Publ. Math. Inst. Hautes Études Sci.* **122** (2015), 65–168.
[22] M. Gross and B. Siebert, ‘From real affine geometry to complex geometry’, *Ann. of Math.* (2) **174**(3) (2011), 1301–1428.
[23] M. Gross and B. Siebert, ‘An invitation to toric degenerations’, in *Surveys in Differential Geometry,* Vol. XVI, *Geometry of Special Holonomy and Related Topics*, Surveys in Differential Geometry, 16 (Int. Press, Somerville, MA, 2011), 43–78.
[24] C. Haase and J. Schicho, ‘Lattice polygons and the number $2i + 7$’, *Amer. Math. Monthly* **116**(2) (2009), 151–165.
[25] P. Hacking and Y. Prokhorov, ‘Smoothable del Pezzo surfaces with quotient singularities’, *Compos. Math.* **146**(1) (2010), 169–192.
[26] N. O. Ilten, ‘Mutations of Laurent polynomials and flat families with toric fibers’, *SIGMA Symmetry Integrability Geom. Methods Appl.* **8** (2012), 47–53.
[27] A. M. Kasprzyk, ‘Bounds on fake weighted projective space’, *Kodai Math. J.* **32** (2009), 197–208.
[28] A. M. Kasprzyk, M. Kreuzer and B. Nill, ‘On the combinatorial classification of toric log del Pezzo surfaces’, *LMS J. Comput. Math.* **13** (2010), 33–46.
[29] J. Kollár and N. I. Shepherd–Barron, ‘Threefolds and deformations of surface singularities’, *Invent. Math.* **91**(2) (1988), 299–338.
[30] M. Kontsevich and Y. Soibelman, ‘Affine structures and non-Archimedean analytic spaces’, in *The Unity of Mathematics*, Progress in Mathematics, 244 (Birkhäuser Boston, Boston, MA, 2006), 321–385.

Downloaded from https://www.cambridge.org/core. IP address: 185.31.154.38, on 21 Aug 2017 at 16:48:03, subject to the Cambridge Core terms of use, available at https://www.cambridge.org/core/terms. https://doi.org/10.1017/fms.2017.10

[31] J. C. Lagarias and G. M. Ziegler, 'Bounds for lattice polytopes containing a fixed number of interior points in a sublattice', *Canad. J. Math.* **43**(5) (1991), 1022–1035.
[32] K. Mahler, 'Ein Übertragungsprinzip für konvexe Körper', *Časopis Pěst. Mat. Fys.* **68** (1939), 93–102.
[33] T. Mandel, 'Classification of rank 2 cluster varieties', Preprint (2014), arXiv:1407.6241 [math.AG].
[34] M. Perling, 'Combinatorial aspects of exceptional sequences on (rational) surfaces', Preprint (2013), arXiv:1311.7349 [math.AG].
[35] G. A. Pick, 'Geometrisches zur zahlenlehre', *Sitzungber Lotos* **19** (1899), 311–319.
[36] T. Prince, 'Smoothing toric Fano surfaces using the Gross–Siebert algorithm', Preprint (2015), arXiv:1504.05969 [math.AG].
[37] S. Rabinowitz, 'A census of convex lattice polygons with at most one interior lattice point', *Ars Combin.* **28** (1989), 83–96.
[38] M. Reid, 'Young person's guide to canonical singularities', in *Algebraic Geometry, Bowdoin, 1985 (Brunswick, Maine, 1985)*, Proceedings of Symposia in Pure Mathematics, 46 (American Mathematical Society, Providence, RI, 1987), 345–414.
[39] P. R. Scott, 'On convex lattice polygons', *Bull. Aust. Math. Soc.* **15**(3) (1976), 395–399.
[40] M. Symington, 'Four dimensions from two in symplectic topology', in *Topology and Geometry of Manifolds (Athens, GA, 2001)*, Proceedings of Symposia in Pure Mathematics, 71 (American Mathematical Society, Providence, RI, 2003), 153–208.
[41] J. M. Wahl, 'Elliptic deformations of minimally elliptic singularities', *Math. Ann.* **253**(3) (1980), 241–262.

Downloaded from https://www.cambridge.org/core. IP address: 185.31.154.38, on 21 Aug 2017 at 16:48:03, subject to the Cambridge Core terms of use, available at https://www.cambridge.org/core/terms. https://doi.org/10.1017/fms.2017.10